ACS APPLIED MATERIALS & INTERFACES

www.acsami.org

Review

Beyond the Single-Nozzle: Coaxial Electrospinning Enables Innovative Nanofiber Chemistries, Geometries, and Applications

Prerana Rathore and Jessica D. Schiffman*

Cite This: *ACS Appl. Mater. Interfaces* 2021, 13, 48−66

Read Online

ACCESS | Metrics & More | Article Recommendations

ABSTRACT: With an ever increasing scientific, technological, and industrial interest in high surface area, porous nanofiber mats, electrospinning has emerged as a popular method to produce fibrous assemblies for use across biomedical, energy, and environmental applications. However, not all precursor solutions nor complex geometries can be easily fabricated using the traditional single-nozzle apparatus. Therefore, coaxial electrospinning, a modified version of electrospinning that features a concentrically aligned dual nozzle, has been developed. This review will first describe the mechanism of electrospinning two precursor solutions simultaneously and the operational parameters that need to be optimized to fabricate continuous fibers. Modifications that can be made to the coaxial electrospinning process, which enable the fabrication of uniform fibers with improved properties, as well as the fabrication of fibers that are hollow, functionalized, and from "nonspinnable precursors" will be discussed as a means of promoting the advantages of using a coaxial setup. Examples of how coaxially electrospun nanofibers are employed in diverse applications will be provided throughout this review. We conclude with a timely discussion about the current limitations and challenges of coaxial electrospinning.

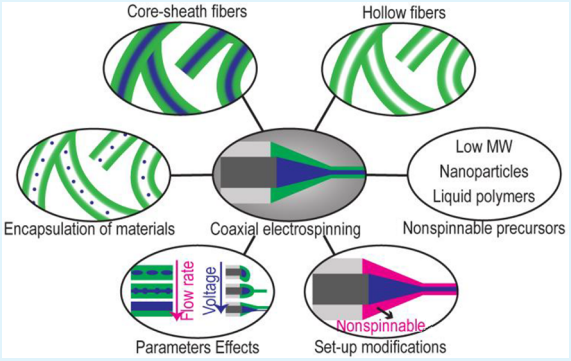

KEYWORDS: *coaxial electrospinning, core−sheath, electrospinning, hollow fibers, nanofibers, polymer*

1. INTRODUCTION

Due to their high surface-to-volume ratio, porosity, and mechanical properties, nanofibers have widespread applications in drug delivery,[1,2] tissue engineering,[3,4] sensors,[5] energy storage,[6,7] and separation membranes.[8,9] While numerous methods can be used to fabricate nanofibers, e.g., template synthesis,[10,11] drawing,[12,13] self-assembly,[14,15] phase-separation,[16,17] and centrifugal spinning,[18,19] only electrospinning[20] is a versatile, cost-effective, and straightforward strategy to provide great control over the fibers' diameters, characteristics, and morphologies. Unfortunately, the simplest single-nozzle setup has limitations; for example, forming fibers from low molecular weight or unentangled polymer solutions is challenging. Notably, a modified version of single-nozzle electrospinning, known as coelectrospinning or, more commonly, coaxial electrospinning, can be used to overcome these limitations.

Although developed less than 20 years ago, coaxial electrospinning has attracted a great deal of attention. The first attempt at using a coaxial setup was reported in 2002 by Loscertales et al.[21] who encapsulated water in oil droplets. A year later, the first successful fabrication of core−sheath nanofibers using coaxial electrospinning was demonstrated by Sun et al.[22] Since these initial studies, coaxial electrospinning has been used to fabricate core−sheath and multilayered fibers in a straightforward one-step manner,[23,24] as well as hollow fibers using a two-step manner.[25,26] Previous review articles have highlighted the applicability of core−sheath fibers.[27,28] Recently, exciting progress fabricating fibers from precursor solutions comprised of low molecular weight polymers and low polymer concentrations has been demonstrated, thus enabling new applications.[29,30]

In this review, we will first provide an overview of the experimental setup and mechanism of single-nozzle (Section 1.1) and coaxial electrospinning (Section 1.2) followed by a discussion of parameters that affect both processes (Section 2). The discussion is followed by three major uses of coaxial electrospinning that overcome limitations of single-nozzle electrospinning, i.e., producing hollow fibers (Section 3), encapsulating cargo with controlled release rates (Section 4), and obtaining fibers from nonspinnable precursors (Section 5). Next, we describe electroblowing (Section 6.1) and liquid-assisted electrospinning (Section 6.2), which are the two major

Received: October 2, 2020
Accepted: December 10, 2020
Published: December 23, 2020

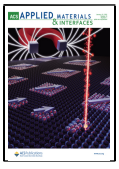

extensions of the coaxial electrospinning process, which further expand the potential application space of coaxially electrospun fibers. Finally, we will conclude this review by providing our perspective about the future potential and limitations of coaxial electrospinning (Section 7).

1.1. Brief Overview of Single-Nozzle Electrospinning. To better understand the coaxial process, we first will provide a brief overview of single-nozzle electrospinning. Typically, the electrospinning process is driven by applying a voltage across a conductive collector and a conductive spinneret that supplies the precursor solution at a desired flow rate (Figure 1A).

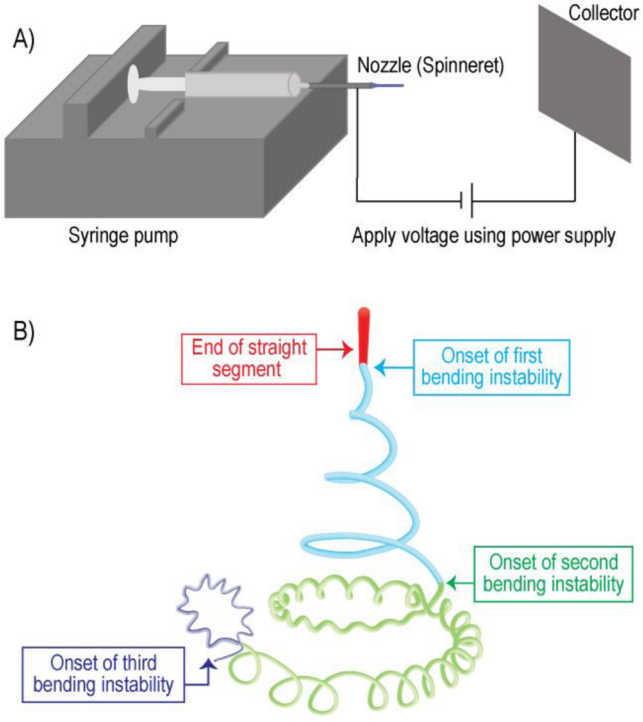

Figure 1. (A) Schematic of a classic single-nozzle electrospinning setup. A spinneret is attached to a syringe filled with a precursor solution that is supplied at a controlled flow rate using an advancement pump. A voltage is applied across the nozzle and collector using a high-voltage power supply. (B) The electrospinning jet undergoes multiple rounds of whipping instability while traveling from the nozzle to the collector. Figure 1B is redrawn with permission from ref 38. Copyright American Chemical Society 2006.

Applied voltage induces charges in the precursor solution so that a charged droplet is generated at the orifice of the spinneret.[20] When the applied voltage is high enough to overcome the surface tension and viscous forces, Coulombic forces stretch the drop into a conical shape, known as the Taylor cone.[31] Next, the charged jet is ejected from the tip of the Taylor cone and travels toward the collector due to the electric field. As the jet travels, it thins due to stretching that results from the repulsion between charges in the jet. Repulsion between charges also causes whipping instability, which increases the path of the jet significantly.[32−35] Multiple rounds of whipping instability can occur during electrospinning (Figure 1B).[33] As the jet travels, it also solidifies due to rapid solvent evaporation, and thus, solid fibers are collected on the conductive collector. The detailed description of single-nozzle electrospinning can be found in many review articles, including those by Reneker and Yarin,[20] Schiffman and Schauer,[36] and Rutledge and Fridrikh.[37]

1.2. Overview of Coaxial Electrospinning. In coaxial electrospinning, the spinneret consists of two nozzles that are concentrically aligned, and the core and sheath precursor solutions are fed at a controlled rate through the inner and outer nozzle, respectively (Figure 2A). At the orifice of the

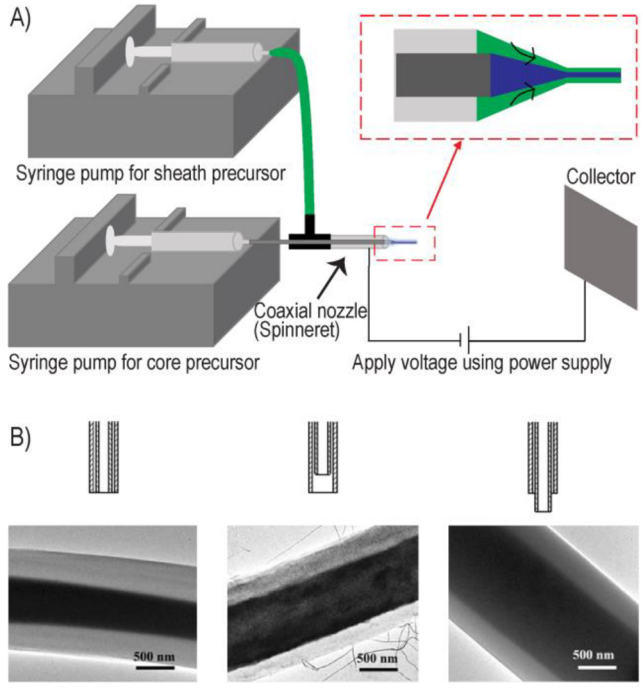

Figure 2. (A) Schematic of the coaxial electrospinning setup. Core and sheath precursors are supplied to a spinneret with two concentric nozzles at controlled flow rates using two different syringe pumps. A voltage is applied across the spinneret and a collector using a high-voltage power supply. (B) The relative alignment of the inner and outer nozzles impacts fiber formation. For example, the bottom right transmission electron micrograph displays that a thicker core and thinner sheath result when the inner nozzle protrudes from the outer nozzle. Figure 2B is reproduced with permission from ref 39. Copyright Springer Nature 2016.

spinneret, a compound droplet is generated, and upon applying voltage, charges are induced in the droplet. The distribution of these charges depends on the electrical conductivity of both the core and sheath solutions, as will be discussed later in the Section 2.3, "***Solutions Properties: Electrical Conductivity***". When an adequate voltage is applied, the sheath precursor is stretched, which imposes a viscous drag force on the core precursor material thus, entraining the core within the sheath. The entrainment is aided by protruding the inner nozzle out from the outer nozzle by half of the radius of the outer nozzle.[40] This stretching and entrainment causes a compound Taylor cone to form from which a compound jet ejects and subsequently undergoes stretching, whipping instability, and solidification− just as described in single-nozzle electrospinning. However, here in coaxial electrospinning, solid core−sheath fibers are formed on the collector. The relative alignment of the inner and outer nozzle affects the entrainment and, consequently, the resulting fiber morphology, as shown in Figure 2B.

https://dx.doi.org/10.1021/acsami.0c17706
ACS Appl. Mater. Interfaces 2021, 13, 48−66

During coaxial electrospinning, the core might offset from the center of the sheath due to a flow instability, such as a whipping instability (Figure 3A).[41,42] In extreme cases, the

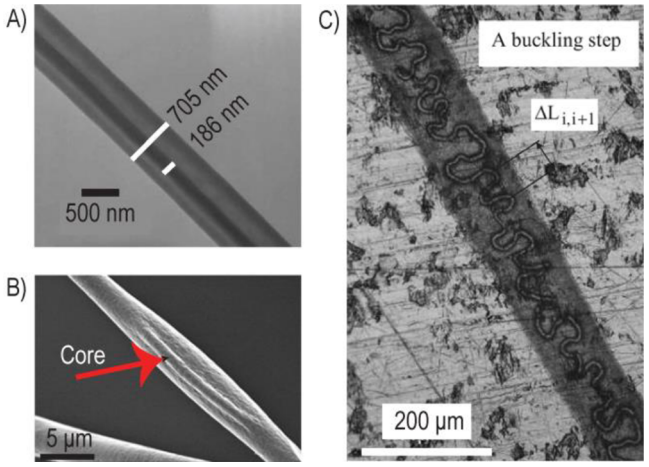

Figure 3. Transmission electron micrographs display (A) a single fiber that has an offset core within a sheath. (B) A core that is not fully enveloped by the sheath thus, exposing the core to the environment. (C) A buckled core is visible within a straight thick fiber sheath. Here, the sheath did not undergo whipping instability, but the core did. Figure 3A is reproduced with permission from ref 41. Copyright Elsevier 2005. Figures 3B and C are reproduced with permission from ref 43. Copyright John Wiley & Sons 2006.

core might be exposed to the environment because it is not fully enveloped by the sheath (Figure 3B).[43] In cases where the core has a higher velocity than the sheath, it is possible that only the core will undergo whipping instability, which results in fibers that have a thick sheath and a buckled core (Figure 3C).[43]

Optimizing the properties of the two precursor solutions is the key to successfully forming fibers. The outer liquid is typically a polymeric solution, while the inner precursor does not need to be; it could be a non-Newtonian suspension of particles or even a Newtonian liquid. When "nonspinnable" precursors are employed in the core, they tend to break up into droplets due to Rayleigh instabilities. Ideally, an elastic sheath can be used to stabilize the core because it suppresses Rayleigh instabilities, as well as strain hardens the core during jetting.[44] Furthermore, the interfacial tension of core−sheath interface is low which, in turn, reduces the driving force for Rayleigh instabilities.[44]

Numerous modifications have been made to the coaxial electrospinning setup. While metric syringe pumps are most commonly used to drive the core and sheath precursors, numerous studies have employed air/gas pressure[22] or simply gravity.[23] Modifications in spinneret designs are also common. For example, Figure 4A shows a setup where a smaller and larger nozzle (containing the core and sheath precursors, respectively) were placed perpendicular to each other, and the collector was held at a fixed distance from the larger nozzle.[45] Next, the tip of the small nozzle was inserted into the droplet at the orifice of the larger nozzle such that a compound droplet formed, which gave rise to a compound Taylor cone. Figure 4B displays a core-cut nozzle system in which a core nozzle is cut short or removed.[46] In this system, the enveloping of the core fluid by the sheath fluid takes place within the sheath nozzle itself. Other modifications to coaxial electrospinning, include

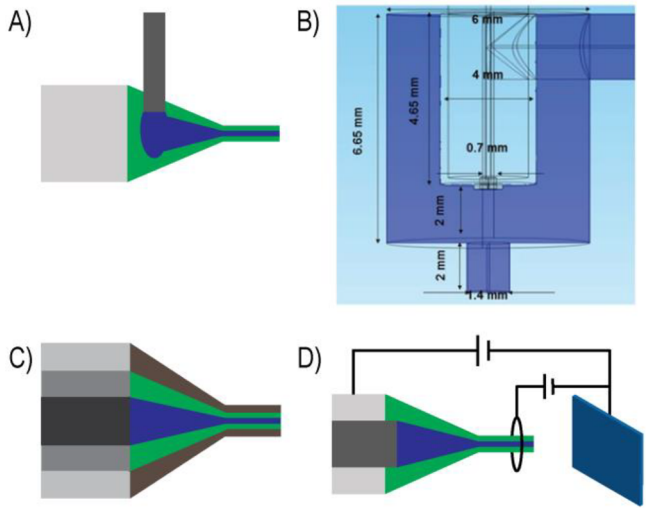

Figure 4. Modified coaxial electrospinning setups. Instead of using two concentrically aligned nozzles, researchers have demonstrated coaxial electrospinning setups using (A) a smaller nozzle that is inserted into a larger nozzle perpendicularly, (B) a core-cut setup in which the core nozzle is shortened or removed, and (C) three concentrically aligned nozzles to enable three-fluid electrospinning. (D) A secondary electric field has been applied via a conductive ring placed between the spinneret and the collector. Figure 4A is redrawn with permission from ref 45. Copyright AIP Publishing LLC 2006. Figure 4B is reproduced with permission from ref 46. Copyright Springer Nature Limited 2015. Figure 4C is redrawn with permission from ref 49. Copyright American Chemical Society 2013. Figure 4D is redrawn with permission from ref 50. Copyright John Wiley & Sons 2015.

using a triaxial nozzle for three-fluid spinning[47−49] (Figure 4C) and adding a second electric field to extend the polymer chains along the fiber's axis[50] (Figure 4D).

2. PARAMETERS THAT AFFECT COAXIAL ELECTROSPINNING

Both single-nozzle and coaxial electrospinning processes are affected by three major categories of parameters: solution properties (i.e., elasticity, viscosity, polymer concentration, electrical conductivity, surface tension), environmental conditions (i.e., humidity, airflow, temperature), and process parameters (i.e., flow rate, voltage, tip-to-collector distance).[51,52] While for single-nozzle electrospinning, only one precursor solution needs to be optimized; coaxial electrospinning typically involves two precursors, and thus, more parameters are involved. In the following sections, our goal is to link how coaxial electrospinning is affected by the same parameters as single-nozzle, yet at times, more complications arise. We will focus on discussing the most important parameters, as an extensive study of the effect of all the parameters is beyond the scope of this review article.

2.1. Solutions Properties: Polymer Concentration. In single-nozzle electrospinning, when the concentration of polymer is below the entanglement concentration, electrospraying occurs, instead of electrospinning. On the other extreme, when the concentration is very high, the viscosity becomes too high for electrospinning to occur because the Coulombic forces are not able to overcome the viscous forces. Many reports indicate that within a spinnable regime for single-nozzle electrospinning, increasing the polymer concentration coincides with an increasing fiber diameter.[53] In general

https://dx.doi.org/10.1021/acsami.0c17706
ACS Appl. Mater. Interfaces 2021, 13, 48−66

for coaxial electrospinning, it has been observed that when the polymer concentration of the sheath precursor is low, the resultant fibers have a beads-on-a-string morphology due to the onset of Rayleigh instability, whereas by increasing the polymer concentration/viscosity of the sheath precursor, the instabilities are suppressed, and smooth fibers are formed.[24,54] Generally, the overall fiber diameter increases with the polymer concentration in the sheath precursor[55,56] (Figure 5A);

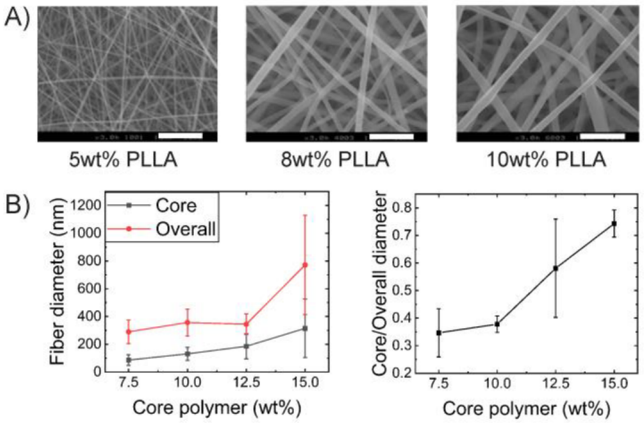

Figure 5. The polymer concentrations in the core and sheath precursor solutions influences the resultant average fiber diameter. (A) Scanning electron micrographs of poly(L-lactic acid) (PLLA) fibers coaxially electrospun as a function of sheath polymer concentration display that their overall diameter increases with increasing sheath polymer concentration. Scale bars are 10 μm. Figure 5A is reproduced with permission from ref 56. Copyright Taylor and Francis Group 2006. (B) Left: As the concentration of the core polymer increases, both the core and the overall fiber diameter increases. Right: The ratio of the core diameter to the overall diameter increases as well. Figure 5B is redrawn with permission redrawn using the data from ref 23. Copyright American Chemical Society 2004.

however, a few exceptions have been demonstrated.[24] The overall diameter of the fibers also increases with the core polymer concentration,[23] see Figure 5B. Li et al.[57] reported that when the polymer concentration in the core was low, the resultant fibers had round cross sections; upon increasing the concentration they became ribbonlike. This behavior is attributed to the difference in volatility and miscibility of core and sheath solutions, and therefore, in the following section, we consider in greater detail the interactions of the two solutions.

2.2. Solution Properties: Miscibility of Polymers and Solvent. Moghe and Gupta[58] mentioned that having a low interfacial tension between the core and sheath is a criteria for coaxial electrospinning. If the core and sheath solutions are miscible with each other, then the interfacial tension between them is negligible. This was investigated by Sun et al.[22] using poly(ethylene oxide) (PEO) in water−ethanol mixtures containing a different dye concentration in the core and sheath solutions. A sharp boundary existed between the core and sheath layers due to the longer polymer/dye diffusion time scale versus the characteristic electrospinning time scale. Numerous researchers reported that the coaxial electrospinning of miscible solutions resulted in smaller diameter core−sheath fibers with distinct interfaces due to the negligible interfacial tension between the solutions.[44] On the other hand, a few studies showed that diffusion between the core and sheath solutions is possible and might even lead to complete mixing.[25,57,59] For example, when Li and Xia[25] spun a polyvinylpyrrolidone (PVP)/ethanol core solution and a mixture of PVP and a titanium alkoxide/ethanol-acetic acid sheath solution, despite removing the PVP postproduction, they generated solid ceramic fibers with high porosities (Figure 6A).

It is possible that the core and sheath solvents are miscible, while both of the solutes are immiscible. Xin et al.[60] obtained core−sheath fibers that had a distinct interface between the core and sheath by using two immiscible polymers, polystyrene (PS) and poly(*p*-phenylenevinylene) (PPV), as the core and sheath, respectively, while the solvents were miscible. On the other hand, when Li and Xia[25] used two immiscible solutes, PS and a mixture of PVP/titanium alkoxide, as the core and sheath, respectively, and obtained porous solid fibers after the polymers were removed. This behavior is attributed to the miscibility of the core and sheath solvents; because the solvents were miscible, they diffused into each other and carried along the PS and PVP. As the solvent evaporated, the concentration of PS and PVP increased, which caused the immiscible polymers to phase separate[25] (Figure 6B). In a third scenario, it is possible that the core and sheath solvents are miscible, yet the core solute precipitates in the sheath solvent. Here, researchers suggested that the core−sheath fibers had a middle layer that contained both the core and sheath polymers.[57] An extreme case is displayed in Figure 6C

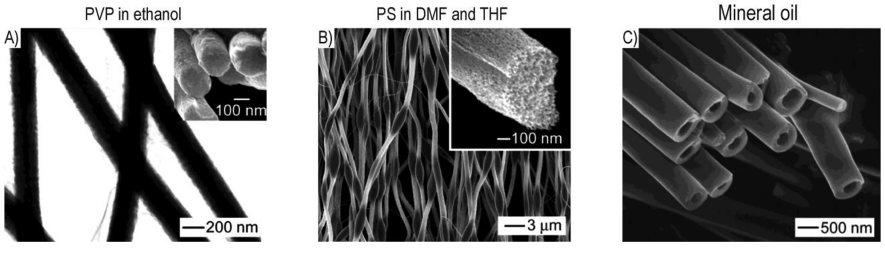

Figure 6. Miscibility of the core and sheath precursor solutions influences the resultant fiber morphology. Transmission electron micrographs display fibers coaxially electrospun using the same sheath solution (titanium alkoxide and polyvinylpyrrolidone (PVP) in a mixture of ethanol and acetic acid) and varied core solutions, including (A) PVP in ethanol, (B) polystyrene (PS) in dimethylformamide (DMF)/tetrahydrofuran (THF), and (C) mineral oil. (A) When the core and sheath precursors were miscible, the two solutions mixed during electrospinning, and solid fibers were produced. (B) When the core polymer was immiscible with the sheath polymer, but the solvents were miscible, first there was solution mixing followed by phase separation of the polymers after the solvents evaporated. The PS rich and PS poor regions inside the PVP-TiO_2 matrix gave rise to porous fibers after the PS and PVP were removed. (C) Hollow fibers were obtained when an immiscible core solution (mineral oil) was employed and removed postspinning. Figures 6A−C are reproduced with permission from ref 25. Copyright American Chemical Society 2004.

https://dx.doi.org/10.1021/acsami.0c17706
ACS Appl. Mater. Interfaces 2021, 13, 48−66

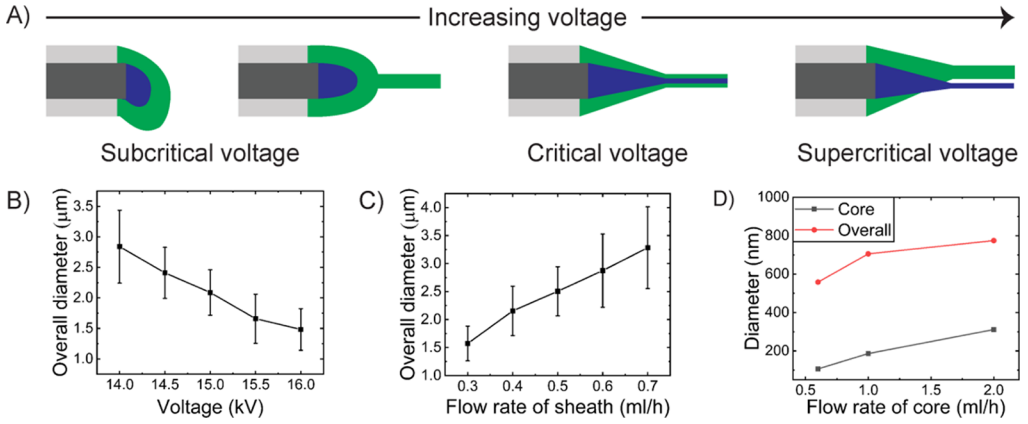

Figure 7. Effect of voltage on coaxial electrospinning. (A) When the voltage is too low (subcritical), the sheath does not entrain the core. By increasing the voltage within a suitable range of critical voltages, a compound and stable Taylor cone forms. At a supercritical voltage, jet splitting is observed. Figure 7A us redrawn with permission based on ref 58. Copyright Taylor and Francis Group 2008. (B) The overall fiber diameter decreases with applied voltage. (C) The overall fiber diameter increases with the flow rate of the sheath. Figures 7B and 7C are replotted with permission based on data from ref 66. Copyright Elsevier 2016. (D) The core and overall diameters of the fibers increase with the flow rate of the core. Figure 7D is replotted with permission based on data from ref 41. Copyright Elsevier 2005.

when two completely immiscible solutions are employed, e.g., mineral oil core with a polymer solution sheath.[25,59,61−64] Many studies have used a combination of immiscible solutions to obtain hollow fibers by removing the core,[25,59,61] as discussed later along with their applications.

2.3. Solutions Properties: Electrical Conductivity. In the compound droplet, the distribution of induced charges depends on the relative electrical conductivity of the core and sheath precursors. If the sheath precursor is more conductive, then the induced charges are located at the sheath-air interface.[65] In this case, the sheath is the driving precursor, and Coulombic forces act on the sheath causing the sheath to entrain the core.[21,65,66] On the other hand, if the core precursor is more conductive, then it acts as the driving precursor and drags the sheath along with it. For example, Loscertales et al.[21] obtained droplets of water coated with olive oil using coaxial electrospraying. Due to insufficient conductivity, olive oil cannot be electrosprayed solo; however, when olive oil was used as the sheath and a conductive liquid was the core, electrospraying occurred. Yu et al.[44] noted that when the core precursor had a higher conductivity than the sheath, the electric field might "pull" the core faster than the sheath, and some fibers might not have a core−sheath morphology.

2.4. Process Parameters: Voltage. In single-nozzle spinning, when the applied voltage is further increased (above the critical voltage), a higher Coulombic repulsion between charges tends to stretch the jet causing the fiber diameter to decrease.[67,68] On the other hand, as voltage increases, a larger amount of liquid is pulled toward the collector, due to an increased electric field, which tends to increase the fiber diameter.[69,70] Depending on which effect dominates, the diameter may increase or decrease (or even follow nonmonotonic behavior) with voltage.[71]

In the case of coaxial electrospinning, only a small range of applied voltages yields core−sheath fibers.[58] When the voltage is too low, the jet does not form, and liquid is dripped from the spinneret[54,58] (Figure 7A). When the voltage is increased, a jet ejects from the sheath, but it does not entrain the core precursor. When voltage is further increased, a stable jet comprised of both the core and sheath is obtained.[58] At even higher voltages, more solution is pulled by the electric field (than supplied by the flow rate) causing the core and sheath solutions to recede into the spinneret, split up, and form multiple jets.[58,63] The specific range of applied voltages that can be employed for successful coaxial electrospinning depends on properties of precursor solution and other experimental parameters. For example, Yao et al.[66] were able to obtain stable coaxial jets of rose hip seed oil encapsulated within zein protein between the applied voltage range of 14 kV and 16 kV, whereas a voltage range of 7−9 kV was applied to obtain a polydimethylsiloxane (PDMS) fiber core within a PVP sheath by Niu et al.[72] For the range of successful applied voltages (where the jet is stable), increasing the voltage results in a decrease in the core diameter[25] and the overall diameter[54,66] (see Figure 7B), but the sheath thickness does not appreciably change.[25] Higher voltages induce more charges in the polymer solution and also increase the repulsion forces between charges which causes the diameter of the fibers to decrease.[66]

2.5. Process Parameters: Flow Rate. When coaxial electrospinning, it is especially important to optimize the flow rate of each precursor solution. In considering the flow rate of the sheath precursor, faster rates will increase the overall fiber diameter[54,66] (Figure 7C) until an upper limit is reached that causes the core to segment.[25,44,45,63] If the flow rate of the sheath is too low, the core will not be fully encapsulated[45,63,73] or it will break up into droplets.[44] If the flow rate of the core is increased, the thickness of the sheath either decreases[25,74] or does not change significantly.[75] Moreover, the core diameter and the overall fiber diameter increase[25,41,73,76] (Figure 7D) due to the higher supply of the core precursor material[74] and die-swell (i.e., Barus) effects owing to the extrusion of a viscoelastic material.[74,76] On the other hand, if the core solution is not viscoelastic, then altering the core flow rate will not change the overall diameter significantly, because the die-swell effects will be minimized.[77]

3. FABRICATION OF HOLLOW FIBERS VIA COAXIAL ELECTROSPINNING

Hollow fibers have been evaluated for various applications, including photocatalysis,[78,79] sensors (for gas,[55] formaldehyde,[80] hydrogen,[81] ethanol,[82] hydrogen peroxide[83]), micro-

https://dx.doi.org/10.1021/acsami.0c17706
ACS Appl. Mater. Interfaces 2021, 13, 48−66

Table 1. Select Examples of Sheath and Core Precursors Used to Fabricate Hollow Fibers via Coaxial Electrospinning and Their Applications[a]

sheath precursor	core precursor	core removal process	applications
PVP + spin-on-glass intermediate solution	motor oil	calcination	single molecule detection[45]
titanium alkoxide + PVP	mineral oil	calcination	gas sensor; Li-ion batteries[55,61,105]
PAN	mineral oil	immersion in hexane	nanofiltration[62]
ammonium metatungstate hydrate + PVP + PS colloidal particles	mineral oil	calcination	hydrogen sensor[81]
titanium-niobiuam oxide ($Ti_2Nb_{10}O_{29}$) + PVP	mineral oil	calcination	anode in lithium ion batteries[106]
PVP + indium nitride	paraffins	calcination	formaldehyde sensor[80]
PVP + tin chloride dihydrate	paraffins	calcination	ethanol sensor,[82] hydrogen peroxide sensor[83]
PVP + titanium *n*-butoxide	PVP and/or silver nanoparticles	calcination	photocatalysis[78,79]
polybutylene terephthalate (PBT) + polypyrrole (PPy)	PVP	sonication in water	micro solid phase extraction[84]
PVDF-HFP	PVP	washed with water	water filtration[86]
PVP + cobaltous acetate	PVP	annealed at high temperature	anode in lithium ion batteries[107]
titanium alkoxide + PVP	PEO	calcination	photocatalysis[108]
titanium alkoxide + PVP	PEO	calcination	lithium-ion batteries[109]
PAN	PMMA	heating	lithium-sulfur batteries[91]
PAN or PAN + SAN	SAN	heating	lithium-ion batteries[87−89]
ammonium tetrathiotungstate + PAN	SAN	two-step heating	electrocatalyst[110]
PCL + ketoconazole + iron oxide nanoparticles	dimethyl silicone oil	perfuse automatically	antimicrobial treatment[94]
cupric nitrate + cobalt acetate + PAN	PAN	calcination	electrocatalyst for zinc-air batteries[90]

[a]Abbreviations: polyacrylonitrile (PAN), polycaprolactone (PCL), poly(ethylene oxide) (PEO), poly(methyl methacrylate) (PMMA), polystyrene (PS), poly(vinyl alcohol) (PVA), polyvinylpyrrolidone (PVP), poly(vinylidene fluoride-*co*-hexafluoropropylene) (PVDF-HFP), styrene-*co*-acrylonitrile (SAN).

solid phase extraction,[84] separation membranes (for nanofiltration,[62] ultrafiltration,[85] water purification[86]), energy applications (including lithium-ion batteries,[87−89] electrocatalysts for zinc-air batteries,[90] lithium-sulfur batteries[91]), tissue engineering,[92,93] single molecule detection,[45] and antimicrobial treatment[94] (see Table 1). There are a number of different techniques—template synthesis,[95,96] self-assembly,[97,98] emulsion electrospinning,[99,100] and coaxial electrospinning[25,61] —that can be used to fabricate hollow nanofibers. Among these methods, coaxial electrospinning provides a straightforward two-step method to fabricate hollow fibers by (i) spinning core−sheath fibers and then (ii) extracting the sacrificial core, which can be nonpolymeric or polymeric. Commonly used nonpolymeric cores include mineral oil,[25,55,59,64] olive oil,[26] and silicon oil.[101] PVP is the most commonly used sacrificial core polymer because it is water-soluble and degrades at lower temperatures.[78,84−86] Additional polymers which have been used as sacrificial cores are poly(methyl methacrylate) (PMMA),[43,91] polypropylene carbonate (PPC),[102] PEO,[85,103] polyethylene glycol (PEG),[93] polyacrylonitrile (PAN),[90] and PS.[104]

The first successful attempts to fabricate hollow fibers via coaxial electrospinning were made in 2004 by Loscertales et al.[26] and by Li and Xia.[25] Loscertales et al.[26] combined the sol−gel technique with coaxial electrospinning by using a tetraethyl orthosilicate (TEOS) sol precursor as the sheath and olive oil or glycerin as the core. Li and Xia[25] obtained hollow silica fibers and investigated the effect that the miscibility of the core and sheath had on obtaining hollow fibers (Figure 6), as discussed in Section 2.2, "***Solutions Properties: Miscibility of Polymers and Solvents***".

The fiber's core can be removed by dissolution in an appropriate solvent or by thermal treatment. For example, mineral oil cores have been removed by immersing the as-spun fibers in solvents including octane[25,63,64] and *n*-hexane[62] or by calcination.[25,55] Similarly, polymeric cores (e.g., PVP) can be removed by calcination or washing. Bagheri et al.[84] obtained hollow polybutylene terephthalate (PBT)/polypyrrole (PPy) fibers by using PVP as a sacrificial core that was removed by sonication in double distilled water for 10 min. Similarly, Ou et al.[93] rinsed away a sacrificial PEG core with water to reveal hollow poly(L-lactic acid) (PLLA) fibers. Pakravan et al.[103] obtained hollow chitosan fibers by immersing the as-spun fibers in water for 24 h to remove the PEO core.

For many systems, it is necessary to stabilize the as-spun core/sheath fibers before removing the core. For example, Chang et al.[78] prepared TiO_2 nanofibers using PVP as the core and titanium *n*-butoxide (TBT) as the sheath. The sheath precursor was prepared by mixing TBT with PVP, acetic acid, and ethanol, and the core precursor was prepared by dissolving PVP in a mixture of ethanol and water. To make sure that the hydrolysis of TBT was complete, the as-spun fibers were kept in wet air for 1 h before the PVP core was removed by calcination in air at 550 °C for 3 h. While the final hollow TiO_2 fibers had an overall diameter of ∼160 nm, before calcination the fibers had an overall diameter of 200 nm. The diameter shrinkage was attributed to the loss of PVP, as well as the transformation of amorphous TiO_2 to a crystalline phase.

If the sheath cannot sustain atmospheric pressure, the hollow fibers have been reported to collapse after core extraction.[63,86] For example, Halaui et al.[86] observed that hollow poly(vinylidene fluoride-*co*-hexafluoropropylene) (PVDF-HFP) fibers collapsed and buckled after core removal. Chan and Kotaki[63] obtained hollow PMMA fibers after using mineral oil as a sacrificial core, which was extracted by socking the fibers in octane for 12 h. While holding the sheath flow rate constant (1 mL/h), they observed that when the core feed rate was 0.4 mL/h, a fraction of hollow fibers collapsed and became

https://dx.doi.org/10.1021/acsami.0c17706
ACS Appl. Mater. Interfaces 2021, 13, 48−66

Table 2. Select Examples of Precursors Used to Fabricate Fibers via Coaxial Electrospinning and Their Release Profile Biomedical Application[a]

sheath precursor	core precursor	release profile	application
PLLA in DMF + chloroform	tricalcium phosphate nanoparticles + PLLA in DMF + chloroform	sustained release for long time; no burst release	bone tissue engineering[114]
PLGA + MNA in DMF + trichloromethane	NAR + PVP in ethanol + DMF	burst release of both NAR and MNA; sustained release for NAR	guided tissue regeneration[115]
PLLA in TFE	cefotaxime sodium in water	biphasic drug release	antimicrobial[135]
PCL-PEG + PCL in chloroform + methanol	basic fibroblast growth factor (bFGF) in PVA	different release profiles	diabetic ulcers[136]
gelatin in water + TFE	MNA + PCL in TFE	biphasic	guided tissue regeneration[137]
PLLCL + gelatin in HFIP	EGF + insulin + hydrocortisone + retinoic acid + BSA	no burst release	wound healing for skin tissue engineering[138]
silk fibroin in formic acid	PVA + rosuvastatin in formic acid	biphasic	enhancing osteogenesis[139]
cellulose acetate + gelatin in acetic acid	PEG + amoxicillin	no burst release	gastrointestinal tract[140]
PCL in DCM + ethanol	BSA in water	initial-burst release	tissue engineering[141]
PCL in TFE	dipyridamole (DIP) + PCL in TFE	biphasic	antiplatelet treatment to reduce risk of the stroke[142]
PCL	fibroblast growth factor (FGF-2) + BSA + PEO	triphasic	promoting fibroblast proliferation for tissue regeneration[143]
r-PEI-HA PCL in chloroform + methanol	pDNA + PEG in water	initial-burst release (4 phases)	tissue engineering[144]
Nylon6 in formic acid	ampicillin + ethanol mixed with PMMA + chloroform	three-stage releases	antibacterial[145]
PLGA in HFIP	nerve growth factor + PEG in water	initial-burst release followed by sustained release	peripheral nerve regeneration[146]
collagen + silver NPs in HFIP	PCL + vitamin A palmitate in DCM	initial-burst release followed by sustained release	wound dressing[147]
PEO in water mixed with flurbiprofen in ethanol	silk + collagen + PEO + vancomycin	first order followed by Fickian diffusion	wound healing[148]
PCL in DCM + DMF	vancomycin hydrochloride + PVP + graphene oxide in water + DMF	biphasic release	antimicrobial[149]

[a]Abbreviations: bovine serum albumin (BSA), dichloromethane (DCM), dimethylformamide (DMF), epidermal growth factor (EGF), hexafluoroisopropanol (HFIP), metronidazole (MNA), naringin (NAR), polycaprolactone (PCL), polyethylene glycol (PEG), poly(ethylene oxide) (PEO), poly(L-lactic acid) (PLLA), poly(L-lactic acid)-*co*-poly-(e-caprolactone) (PLLCL), poly(lactic-*co*-glycolic acid) (PLGA), poly(vinyl alcohol) (PVA), polyvinylpyrrolidone (PVP), tetrafluoroethylene (TFE), tetrahydrofuran (THF).

ribbonlike after the core was removed. The collapse was attributed to the failure of the PMMA sheath to support the small hollow interior. However, when the core rate was increased to 0.6 mL/h, the hollow fibers had a tubular cross section.

The core removal processes can be used to simultaneously change the physical and chemical properties of the fibers. For example, when as-spun fibers that had a sheath of amorphous titanium alkoxide were calcined, not only was the core removed but also the sheath was converted to the anatase crystalline phase of TiO_2.[25,47,59,78] By using a blend of polymers in the sheath solution and selectively removing one of them (while the core was simultaneously removed), hollow fibers with porous walls can be obtained.[73,108] For example, improved catalytic activity was observed after Zhang et al.[108] fabricated hollow nanofibers that were porous after calcination. Di et al.[73] coaxially spun hollow zeolite fibers using a mixture of silicate-1-nanoparticles and PVP as the sheath precursor solution and paraffin oil as the sacrificial core. The addition of PVP in the sheath was necessary as silicate-1-nanoparticles alone are not electrospinnable; after calcination, the core layer as well as PVP were removed. The researchers noted that if the amount of sacrificial sheath PVP was too high, then the porous walls would collapse after polymer removal.

Another chemistry that benefits from undergoing high temperature processing is hollow carbon fibers (HCNFs) or hollow carbon fibers with porous walls (PHCNFs), which are envisioned for energy applications.[88] Many studies obtained HCNFs and PHNCFs based on PAN by stabilizing a PAN sheath at lower temperatures followed by carbonization at high temperature.[43,87−89,91,102] In one example, Zussman et al.[43] obtained HCNFs by using PAN as the sheath and PMMA as the sacrificial core; the PAN sheath was stabilized at 250 °C in air and then carbonization occurred at 1100 °C in an inert-nitrogen environment. Diaz et al.[102] obtained PHCNFs by using PPC, which degrades at a much lower temperature of ∼200 °C, as a sacrificial core layer and a blend of PPC and PAN as the sheath layer. Lee et al.[87] noted that core materials, which degrade at lower temperatures (such as PMMA or mineral oil), will be removed before the PAN sheath can be stabilized, causing the hollow fibers to collapse. Hence, Lee et al.[87−89] used styrene-*co*-acrylonitrile (SAN) as the core precursor and PAN or PAN/SAN as the sheath to obtain HCNFs or PHCNFs, respectively. PHCNFs have better electrochemical performance than HCNFs because the presence of the pores improves the charge transfer at the electrolyte-electrode interface.[88] PHCNFs have been demonstrated to have an initial capacity and reversible capacity of 1003 $mAhg^{-1}$ and 61.8%, respectively, while HCNFs have 653 $mAhg^{-1}$ and 53.9%, respectively.[88]

In a straightforward manner, coaxially electrospun hollow and porous fibers have been functionalized using nanoparticles, enzymes, or other molecules to improve their application potential.[61,79,111] Chang et al.[79] deposited silver nanoparticles onto the inner surface of TiO_2 hollow fibers by using a mixture of PVP and silver nanoparticles as the core and a mixture of

https://dx.doi.org/10.1021/acsami.0c17706
ACS Appl. Mater. Interfaces 2021, 13, 48−66

titanium *n*-butoxide and PVP as the sheath solution. The resulting core−sheath fibers were calcined which resulted in hollow and porous fibers coated with silver nanoparticles. The charge transfer efficiency of such TiO_2-metal composites was improved due to a shift in the Fermi level to a more negative potential, and their photocatalytic activity was enhanced compared to nonfunctionalized hollow TiO_2 fibers. Hollow TiO_2 fibers whose inner surface was independently functionalized with iron oxide nanoparticles were demonstrated by Li et al.[61] by adding a sacrificial oil-based ferrofluid to the core liquid that functionalized the inner surface of the nanofibers during calcination.

3.1. One-Step Coaxial Electrospinning of Hollow Fibers. It is also possible to obtain hollow fibers using a one-step coaxial electrospinning process.[92,112,113] Dror et al.[112] observed that as-spun fibers were hollow when a polycaprolactone (PCL) sheath and PEO core were coaxially spun. The PEO deposited as a thin inner coating on the PCL sheath leaving a hollow center. Here, the sheath polymer was not soluble in the core solvent, and thus, it precipitated when they made contact. Also, during electrospinning, the sheath solvent evaporated much faster, and therefore, the sheath solidified before the core (thus, a wet core was surrounded by a solid sheath). As the evaporation of the core solvents occurs, the volume of the core decreases and either (i) the core will form a solid detached tube from the sheath or (ii) the core will adhere to the inner surface of the sheath if the core polymer tends to wet the sheath; for example, PEO wets PCL. Hence, two immiscible polymeric precursor solutions with more volatile sheath precursors lead to as-spun hollow fibers if the wetting properties are adequate. Similarly, when Na et al.[113] used polyvinylidene fluoride (PVDF) dissolved in an acetone/dimethyl sulfoxide (DMSO) mixture and poly(vinyl alcohol) (PVA) dissolved in an ethanol/DMSO mixture as the sheath and core, respectively, coaxial electrospinning resulted in hollow as-spun fibers because PVDF is not soluble in ethanol. The limitation of this process arises from the strict solvent selection restrictions.

4. ENCAPSULATING CARGO USING COAXIAL ELECTROSPINNING ENABLES APPLICATIONS

Coaxial electrospinning is a facile method to encapsulate a wide variety of cargo into large area textiles. Drugs, proteins, and living cells can be delivered from biocompatible polymers for tissue engineering,[114,115] controlled drug delivery,[116] and antibacterial applications[54] (see Table 2). Self-healing polymer coatings and self-repairing cracks[117−121] can also be achieved by well-designed core−sheath fibers. Phase-change materials (PCMs),[122−127] nanoparticles,[128] and liquid crystals[129,130] have also been encapsulated and explored for thermal energy storage, battery applications, and basic scientific investigations. Previous review papers have thoroughly described the use of coaxially electrospun nanofibers for biomedical applications,[131−134] so we will only briefly touch on those applications. In the following sections, we will highlight specific applications achieved by encapsulating active agents within coaxial fibers.

4.1. Biomedical Applications. When single-nozzle electrospinning is used for drug encapsulation, a blend of drug and polymer is often used as the precursor solution, which dictates that they must be adequately miscible and that the solvent should not degrade the drug (Figure 8A). Coaxial electrospinning avoids these issues because generally the drug

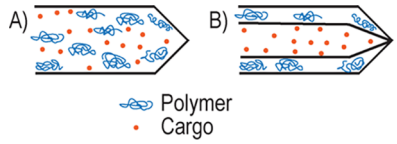

Figure 8. Encapsulation of cargo via (A) single-nozzle and (B) coaxial electrospinning. (A) In single-nozzle electrospinning, the encapsulated material is blended with an electrospinnable polymeric solution. (B) In coaxial electrospinning, the encapsulated cargo can be placed in the core to mitigate contact with sheath solvents.

is incorporated in the core via a compatible solvent, and a different solvent can be employed for the sheath[150] (Figure 8B). Due to the fast electrospinning process, the sheath solvent, even if incompatible with the drug, does not typically affect the drug's performance. Another advantage of releasing drugs from the core of core−sheath fibers is that the sheath decreases the diffusion rate, and a sustained drug delivery can be achieved;[114] this opposes the initial-burst release common in single-nozzle electrospun fibers.[151] For example, He et al.[151] fabricated aligned core−sheath fibers that were comprised of the antibiotic tetracycline hydrochloride (TCH) as the core and the biodegradable FDA-approved polymer PLLA as the sheath. The resulting core−sheath fibers exhibited a suppressed initial-burst release and released 22.9% of the TCH over 144 h versus the single-nozzle electrospun blended TCH/PLLA fibers that released >30% within 8 h. In another study, by encapsulating either the antioxidant Resveratrol or the antibiotic Gentamycin sulfate into the nontoxic polymer PCL, using coaxial electrospinning, Huang et al.[152] eliminated the initial-burst release of both drugs. Ji et al.[153] encapsulated bovine serum albumin (BSA) protein and BSA-PEG blend in a PCL sheath via coaxial electrospinning. A single-nozzle electrospun blend of BSA-PEG fibers was prepared as a control. They reported that all three fibers had a similar initial-burst release but that the cumulative release by week 5 was slowest from the core-sheath fibers (∼50% release) and fastest from the blended fibers (∼70% release).

Varying the sheath properties, such as hydrophobicity, degree of cross-linking, and thickness, will affect the release profile.[154] Moreno et al.[154] encapsulated the enzyme lactate dehydrogenase inside a cross-linked PVA sheath that was stable after being immersed in water for 3 days. A faster release of an anti-HIV drug named maraviroc was achieved by Ball et al.[150] when a lower surface tension media was employed because the fibers were wet efficiently. Notably, the pH value of the release media affects the release rate; it was slower in a basic medium compared to acidic. This behavior is attributed to the fact the deionization of maraviroc depends on the pH value, and it becomes hydrophobic above a pK_a of 7.8.

By loading drugs with varying hydrophilicities in different layers of core−sheath fibers, optimized release profiles can be achieved for each compound. For example, He et al.[115] loaded naringin (NAR), a hydrophilic compound that promotes tissue regeneration in the core, and metronidazole (MNA), a hydrophobic antibiotic that works well against anaerobic bacteria in the sheath layer of their fibers. The MNA in the sheath released faster than the NAR, which exhibited a sustained release; these fibers inhibited bacterial infections while also promoting MC3T3-E1 cell growth and guided tissue regeneration. The antibacterial efficiency of fibers was assessed against *Fusobacterium nucleatum* using the Kirby-Bauer

https://dx.doi.org/10.1021/acsami.0c17706
ACS Appl. Mater. Interfaces 2021, 13, 48−66

method. As the concentration of MNA in fibers increased, the zone of inhibition also increased (Figure 9).

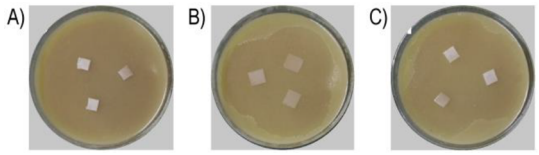

Figure 9. Antibacterial activity of core−sheath fibers containing metronidazole (MNA) in the sheath layer and naringin (NAR) in the core layer. As the concentration of MNA increases, the zone of inhibition increases. (A) Control core−sheath fibers that do not contain any drugs. (B) Fibers electrospun from the sheath precursor containing 0.2 w/v % MNA and the core precursor containing 0.7 w/v% NAR. (C) Fibers electrospun from the sheath precursor containing 0.4 w/v % MNA and the core precursor containing 1.5 w/v% NAR. Figures 9A−C are reproduced with permission from ref 115. Copyright Elsevier 2018.

Encapsulation of living cells is important for tissue regeneration, microbiome, and gene delivery.[155,156] Townsend-Nicholson and Jayasinghe[157] encapsulated immortalized human astrocytoma (cell line 1321N1) within PDMS fibers. After coaxial spinning, ∼67% of the cells were viable, compared to the ∼70% cell viability that was demonstrated when the precursor solutions were passed through the coaxial spinneret without applying any voltage. Also in PDMS fibers, Jayasinghe et al.[156] encapsulated a starting concentration of up to 10^7 cells/mL of primary porcine vascular smooth muscle cells (PASMCs) or rabbit aorta smooth muscle cells (RASMCs) and observed their long viability.

4.2. Energy, Environment, and Industrial Applications. Due to their thermal energy storage ability, phase change materials (PCMs), such as paraffin and natural wax, are attractive high-performance materials that can absorb energy as latent heat and then release it slowly during solid-to-liquid or liquid-to-gas phase transitions.[122−127] PCMs need to be encapsulated, which can be accomplished by interfacial polymerization,[158,159] coacervation,[160] or other techniques, to protect them from the environment and to avoid leakage during phase-transitioning. Notably, coaxial electrospinning provides a straightforward method to encapsulate PCM into continuous fibers.[122−127] McCann et al.[122] encapsulated a hydrocarbon-based PCM named octadecane in TiO_2 fibers via coaxial electrospinning. To investigate their insulating capacity, a glass vial containing water was heated to 60 °C and then cooled to 4 °C. A noncovered glass vial cooled in 7 min; however, when covered with octadecane-TiO_2 fibers, the cooling time was 16 min (Figure 10). Hu and Yu[123] encapsulated soybean wax, a biobased PCM, in polyurethane (PU) and observed that the thermal enthalpy of the composite fibers increased. When Van Do et al.[124] and Rezaei et al.[126] used PEG as a PCM inside PVDF and cellulose acetate (CA) coaxial fibers, respectively, they demonstrated good thermal stability and energy storage capacity.[124,126] PCMs encapsulated inside hydrophobic sheaths have exhibited an increased stability in a moist environment.[125] Lu et al.[127] incorporated hexagonal cesium tungsten bronze nanoparticles in a core paraffin wax layer to improve the efficiency of solar energy absorption.

Silicon (Si) is one of the most promising anode materials for lithium-ion batteries due to its high theoretical capacity.[128]

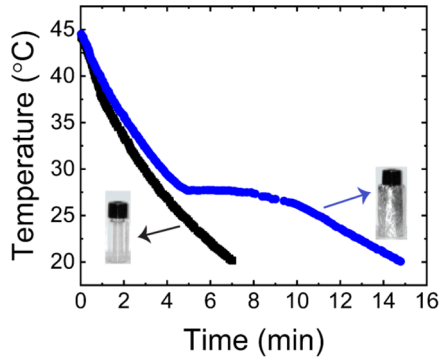

Figure 10. Heat-storage efficiency of core−sheath fiber mats containing PCMs. Glass vials were heated to 60 °C and then allowed to cool down to 4 °C. Without insulation, cooling took 7 min (black curve); however, when the glass vial was fully wrapped with a core−sheath fiber mat containing PCMs, the glass vial took 16 min to cool down (blue curve). Figure 10 is redrawn with permission based on data from ref 122. Copyright American Chemical Society 2006.

However, it has a short life cycle due to many reasons, including the pulverization of Si caused by built-up stresses that are attributed to the expansion and shrinkage of Si volume during cycling. Therefore, nanostructured Si exhibits improved life cycle as it has better stress relaxation due to its small size. However, challenges in producing large-scale nanostructured Si has prevented its use as an anode in Li-ion batteries. Coaxial electrospinning can be implemented for large-scale production of coaxial fibers in which Si nanoparticles are encapsulated by PAN sheath which can be carbonized later.[128] The resulting nanoparticle embedded carbon fibers show outstanding electrochemical performance, and their cycling capacity does not decay significantly for many cycles.[128]

Fertilizers, when encapsulated within a biodegradable polymer, can be controllably released, thus avoiding soil pollution and any harmful effects to plants. Kampeerapappun and Phanomkate[161] encapsulated a mixture of fertilizer and polylactic acid inside polyhydroxybutyrate fibers via coaxial electrospinning. As the flow rate of the core increased, the sheath thickness decreased, which increased the release rate of the fertilizer. The fiber mats released all of the fertilizer within 1 month and completely biodegraded within 3 months.

The ability to repair small cracks, maintain structural integrity, and improve the lifespan of a structure is highly desirable and has been demonstrated using self-healing materials that include polymers and elastomers, as well as metals and ceramics.[162] The most common method involves encapsulating the healing agent inside carriers (capsules[162] or nanofibers[117−121]), which are dispersed in a matrix material. When a crack propagates, the matrix material breaks causing the healing agents to contact a catalyst or curing agent, which heals the crack due to polymerization or cross-linking (Figure 11). Due to their small size and large network, nanofibers are considered a better approach than bulky capsules (∼10 μm), which also can reduce structural stability.[119,121]

5. COAXIAL ELECTROSPINNING FROM NONSPINNABLE PRECURSORS

Coaxial electrospinning enables fiber formation from numerous precursors that are considered "nonspinnable", including Newtonian solutions, low molecular weight/low viscoelasticity polymer solutions, polymeric solutions below the entangle-

https://dx.doi.org/10.1021/acsami.0c17706
ACS Appl. Mater. Interfaces 2021, 13, 48−66

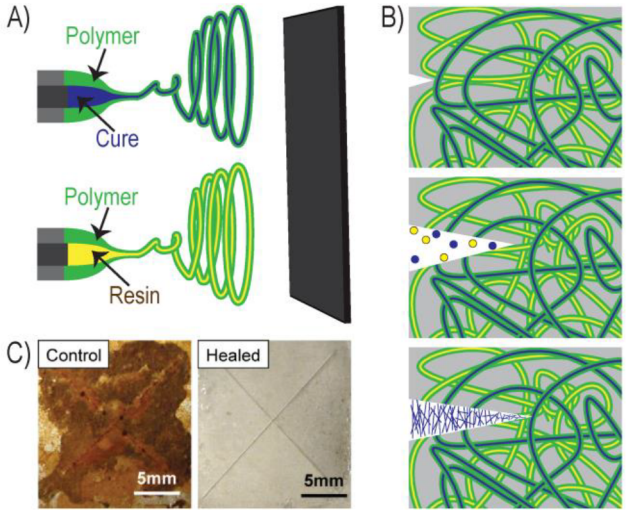

Figure 11. Fabrication of self-healing materials via coaxial electrospinning. (A) The cure and resin are encapsulated simultaneously or sequentially in different fibers via coaxial electrospinning. (B) When a crack propagates, the cure and resin are released from the core–sheath fibers and react with each other leading to curing or polymerization of resin that causes the crack to heal. (C) A cold-rolled steel surface was coated with fibers that contained healing agents and compared to a control surface (no fiber coating). The surfaces were cut using a razor blade and immersed in salt water for 120 h before being stored for 3 months. After 3 months, the coated sample resisted rusting indicating the self-healing capabilities of the fibers. Figure 11C is reproduced with permission from ref 117. Copyright John Wiley & Sons 2010.

ment concentration, and liquid polymers including elastomers. The nonspinnable precursor is fed as the core precursor, and a traditionally spinnable solution is used as the sheath precursor which entrains the core due to viscous drag. The core is stabilized by the presence of the sheath due to strain hardening and lower interfacial tension which suppresses Rayleigh instabilities and eliminates beads-on-a-string morphology.[44] Hence, core–sheath nanofibers are obtained, and if desired, postprocessing (i.e., physical or thermal treatment) can be used to stabilize the core and/or remove the sheath. For example, Sun et al.[22] successfully fabricated fibers from the nonspinnable material palladium acetate, as well as from the low molecular weight polymer poly(dodecylthiophene), by using polylactic acid (PLA) and PEO as the sheath templates, respectively.

The range of spinnable polymer concentrations is also expanded using coaxial electrospinning. For example, in single-nozzle electrospinning, gelatin/tetrafluoroethylene (TFE) does not electrospin at a 2.5 wt % concentration, produces beaded fibers at 5 wt %, and does not form fibers at 12.5 wt %.[163] However, when gelatin/TFE was used as a core solution with PCL/TFE as a sheath, the concentration of spinnable solutions ranged from 2.5 wt % to 20 wt %, and the beads-on-a-string morphology typically observed at lower concentrations was mitigated as the viscoelastic sheath suppressed the Rayleigh instability.[163] Similarly, using coaxial electrospinning, smooth, cylindrical fibers can be obtained from 3 and 5 wt % PAN by using poly(acrylonitrile-*co*-styrene) (PAN-*co*-PS) as a sheath template which was later removed;[44] without the sheath, fibers could not form, and beaded fibers resulted from 3 and 5 wt % PAN solutions, respectively.

PDMS fibers are desirable because the polymer elastomer has vast applications in microfluidics,[164] medicine,[165,166] and sensors[30] due to its inert, nonflammable, nontoxic, biocompatible, and gas-permeable[72] nature. Unfortunately, single-nozzle electrospinning of any liquid polymer is challenging, because the process relies on solvent evaporation.[167] By coaxially electrospinning PDMS/cross-linker as the core precursor and a traditionally "electrospinnable" sheath precursor, stable PDMS fibers can be obtained post-cross-linking; if desired, the sheath can be removed.[30,72,168–170] Coaxial electrospinning also provides an easy method to tune the properties and functions of PDMS fibers. For example, magnetically charged elastic fibers appropriate for sensing applications can be fabricated by mixing magnetic nanoparticles into the PDMS precursor solution.[169] Similarly, PDMS fibers can be used as oxygen sensors for cancer cell research or engineered tissue growth by adding a probe, such as tris(4,7-diphenyl-1,10-phenanthroline)ruthenium(II) or Ru(dpp).[30]

Nanofibers comprised of conjugated polymers can advance the field of nano- and microelectronics due to their electronic and optical properties which results from their conjugated π-bonds along the backbone. Organic solar cells or photovoltaics based on conjugated polymers, such as poly(3-hexylthiophene) (P3HT) mixed with an electron acceptor named [6,6]-phenyl-C61-butyric acid methyl ester (PCBM), have attracted a great deal of attention.[29,171] Unfortunately, electrospinning conjugated polymers is difficult because of their insufficient chain entanglement and their limited solubility in most solvents.[29,57] Single-nozzle spinning of conjugated polymers can be enabled by adding a linear carrier polymer, such as PEO; however, finding a common solvent which dissolves both the carrier and the conjugated polymers is challenging; and the conductivity of resulting fibers is significantly reduced due to the carrier polymer. Coaxial electrospinning enables the fabrication of nanofibers from conjugated polymers, including poly[2-methoxy-5-(2-ethylhexyloxy-1,4-phenylenevinylene] (MEH-PPV), and a blend of conjugated polymers such as MEH-PPV and P3HT.[57] Sundarrajan et al.[29] and Bedford et al.[171] have fabricated P3HT:PCBM nanofibers by using an electrospinnable polymer, i.e., PVP or PCL, as a sacrificial sheath layer. By depositing the P3HT:PCBM fibers on a bulk heterojunction, Bedford et al.[171] devices had an improved power conversion efficiency.

6. COAXIAL ELECTROSPINNING OF NONSPINNABLE SHEATH SOLUTIONS

There are two additional modifications to the conventional coaxial apparatus that capitalize on using "nonspinnable" sheath solution[78,172] to enable fiber formation, which we will refer to as electroblowing and liquid-assisted electrospinning (LAES). In electroblowing, which is sometimes called gas-assisted electrospinning, a gas is fed through the outer nozzle of the coaxial spinneret,[173,174] and resulting fibers are single-layered as would have been obtained via single-nozzle electrospinning. In LAES, the sheath precursor is a non-electrospinnable liquid[175] such as a pure solvent or mixture of solvents,[172,176–183] a salt solution,[184,185] and a surfactant solution[186,187] (Figure 12) and also results in single-layered fibers. However, LAES has been extended to include other nonspinnable liquids such as a dilute polymeric solutions[188] as sheaths, and in this case, the resulting fibers are core–sheath. The presence of a gas or solvent is helpful when working with high viscosity precursor solutions that tend to clog the nozzle,

https://dx.doi.org/10.1021/acsami.0c17706
ACS Appl. Mater. Interfaces 2021, 13, 48–66

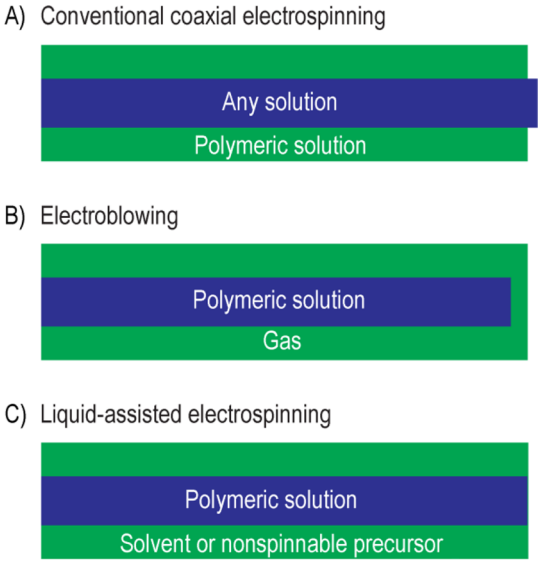

Figure 12. Schematic displaying the differences between (A) conventional coaxial electrospinning, (B) electroblowing, and (C) liquid-assisted electrospinning (LAES) setups. (A) In conventional coaxial electrospinning, the inner nozzle generally protrudes out from the outer nozzle, and the flow rate of the sheath should be higher than the core to facilitate core encapsulation. The sheath precursor is required to be electrospinnable. (B) In electroblowing, the sheath precursor is a gas. (C) In LAES, the inner nozzle sits within the outer nozzle by at least 1 mm. The flow rate of the core precursor is higher than the flow rate of the sheath, which can be a nonspinnable solvent or a dilute polymer solution.

and it also improves the quality of the fiber morphology (i.e., continuous and smooth fibers).

Notably, the mechanism of electroblowing is very different from LAES. In electroblowing, due to the flow of the gas, there is an additional shear force acting on the polymer jet. Upon applying a voltage, the induced charges migrate to the gas−liquid interface, and thus, the liquid is pulled toward the collector by the electric field, as well as by shear forces. In contrast, during LAES the induced charges migrate to the core−sheath interface or to the sheath's surface depending on the relative electrical conductivity of the core and sheath precursors. Moreover, during LAES, the sheath solution continuously evaporates thus making this process more complicated than electroblowing. Nonetheless, both modified processes have been successfully used to obtain smooth and uniform nanofibers. The benefits of electroblowing and LAES can also be transferred to multilayered fibers by using a triaxial nozzle (where the outermost nozzle delivers the gas[189] or solvent[190]). In the sections below, notable examples of electroblowing and LAES will be provided.

6.1. Electroblowing. Electroblowing combines electrospinning with melt blowing by attaching an air or gas blowing unit to a single-nozzle electrospinning setup[191] or by flowing a gas through the outer nozzle of a coaxial spinneret.[173,174] In coaxial electroblowing, due to the gas flow acting on the jet, there is a shear force in addition to the forces typically present during single-nozzle electrospinning.[174,192−194] Importantly, due to additional drag force from the gas flow, more liquid is pulled into the jet, the feed rate of the polymer solution can be increased, and the Taylor cone is stabilized to facilitate a ∼10 times greater production of fibers than single-nozzle electrospinning.[195,196] Typically, electroblown fibers are smaller than those obtained from single-nozzle electrospinning,[193] and the diameter further decreases as the gas flow rate increases.[174,192,193] This is especially true at lower voltages because the jet diameter, and consequently, the contact area, is larger which leads to higher shear forces.[194] On the other hand, at higher applied voltages, single-nozzle electrospinning results in smaller diameters, and hence, the effect of the gas-induced shear force decreases as the voltage increases.[194] Many studies have reported that the flow of gas or dry air aids in evaporating the solvent from the precursor solution.[196,197] For example, when Liu et al.[196] employed a low flow rate of nitrogen gas, the solvent did not fully evaporate, and an interconnected mesh of fibers was obtained on the collector. However, at increased gas flow rates, evaporation from the core precursor increased which reduced the number of interconnected junctions significantly (Figure 13). However, contradicting results, including a lower evaporation of solvent in the presence of gas has also been reported.[192]

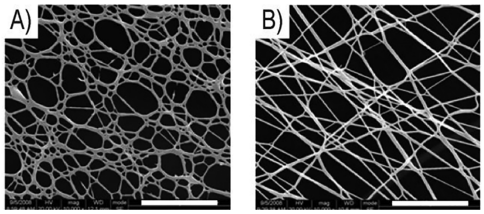

Figure 13. Scanning electron micrographs display the effect that the gas flow rate used during electroblowing has on fiber morphology. (A) At a lower gas flow rate of 2.5 L/min, the fibers are interconnected or weblike, whereas (B) at an increased rate of 10 L/min, the number of interconnected junctions significantly decreases. The scale bars are 10 μm. Figure 13A and 13B are reproduced with permission from ref 196. Copyright Springer International Publishing AG 2009.

By supplying nitrogen gas saturated with dichloromethane (DCM) through outer nozzle, Larsen et al.[173] avoided spinneret clogging and obtained continuous PLA fibers. The flow of saturated gas might have allowed the core precursor to undergo Rayleigh instability by prolonging the core solidification process. Balogh et al.[198] failed at single-nozzle electrospinning nanofibers from a drug (diclofenac sodium) using a carrier named 2-hydroxypropyl-β-cyclodextrin (HPβCD) dissolved in ethanol due to the nozzle clogging from the high volatility solvent. Switching to an ethanol/dimethylformamide mixture slowed the evaporation rate, yet only discontinuous and/or beaded fibers were fabricated. However, when the researchers used a coaxial spinneret featuring an outer nozzle that blew air, continuous fibers were obtained. The additional elongational force from the air flow through the outer nozzle of a coaxial spinneret enabled Zhmayev et al.[199] to overcome the cohesive forces to reduce the agglomeration of nanoparticles in polymeric fibers compared to those spun using a single-nozzle system. The fibers' potential as an anode in Li-ion batteries exhibited a 25% increase in current rate capacity compared to fibers obtained via single-nozzle electrospinning. Paajanen et al.[200] used electroblowing to fabricate zirconium oxide fibers; compressed air was advanced via the outer nozzle, and the inner precursor solution was a blend of PVP and zirconyl chloride octahydrate. The as-electroblown fibers were calcined at different temperatures to control their morphology and crystallinity. Fibers that were calcined at 500 °C had the highest content of the

https://dx.doi.org/10.1021/acsami.0c17706
ACS Appl. Mater. Interfaces 2021, 13, 48−66

tetragonal crystalline phase and exhibited the highest antimonate uptake and adsorption capacity demonstrating their potential to be used to remediate industrial wastewater.

6.2. Liquid-Assisted Electrospinning (LAES). LAES has a few advantages over single-nozzle electrospinning. While high polymer concentration (and in-turn high viscosity) precursor solutions clog single-nozzle electrospinning spinnerets, in LAES, clogging is inhibited because the sheath solvent first works as a lubricant before it slows down the core solvent evaporation rate, which mitigates the formation of a solid skin at the droplet surface.[172,176,179] LAES increases the range of polymer concentrations that can be spun.[172,176] For example, while fibers are not spinnable from very high concentration precursor solutions, including 35% w/v PVP/ethanol (MW = 360 kg/mol)[172,176] or 30% w/v Eudragit L-100/ethanol (MW = 135 kg/mol),[172] LAES has been demonstrated to spin these solutions into small diameter fibers. In fact, much finer fibers are formed using LAES, because the process slows the evaporation of the core liquid to allow the jet to stretch more and undergo more rounds of whipping instability before solidification.[172,176−179]

Of course the volatility and miscibility of core and sheath should be considered. The volatility determines how long the core precursor remains in a liquid state.[178] If the sheath is too volatile, then it defeats the purpose of using LAES because the sheath evaporates too quickly. If the sheath solvent volatility is low, then enough time is granted for the jet to undergo whipping instability. The stretching of the core during whipping instability is supported by the elasticity of the core. However, because nonelastic sheath materials cannot stretch, the sheath breaks up into multiple segments. If the sheath solvent is miscible with the core, then local mixing of the sheath and core results in an uneven polymer concentration, and a wide distribution of fiber diameters is obtained.[172,178,179] Additionally, if the polymer concentration in the segments falls below the entanglement concentration due to mixing, those segments will have beads. In extreme cases, the solvent in the core might not evaporate until the fibers reach the collector. To obtain smooth and uniform fibers, the sheath solvent should evaporate before the onset of the second round of whipping instability.[178]

If the sheath material has a high electrical conductivity, then the amount of charge induced is high, which increases the Coulombic repulsion between the charges and further stretches the jet, thus the fibers have a thinner diameter.[184,185] In contrast, if the jet is pulled faster toward the collector by the electric field (which allows the sheath material to retain for multiple rounds of whipping instability), then the fibers are typically uneven and have a larger diameter.[178,185] The effect of applied voltage was studied by Zhou et al.[201] who observed that by increasing voltage, the height of the Taylor cone decreased, while the half angle of the cone increased. Also, the length of the straight jet (before the onset of bending instability) decreased with voltage.[201]

Unlike conventional coaxial electrospinning, in LAES, the flow rate of the sheath is lower than that of the core.[45,63,73] As the flow rate of the sheath increases, the onset of whipping instability becomes quicker, i.e., whipping instability starts earlier, and the length of the straight jet decreases.[177] Additionally, the envelope cone of whipping instability becomes wider.[177] The diameter of the fibers decreases with the increasing sheath flow rate because the jet remains in a liquid state for a longer time.[172,177] When the flow rate of the sheath is high (close to the core flow rate), the sheath breaks into segments and gives rise to fibers with nonuniform diameters.[172]

The LAES process produces bead-free fibers from precursor solutions, because the Rayleigh instability is suppressed as the surface tension of the core−sheath interface is lower than the liquid−air interface in single-nozzle electrospinning. Surfactant can also be added to decrease the surface tension and apparent viscosity, while increasing the conductivity, all of which result in thinner fibers. However, the same changes increase the rate of evaporation of the solvent and therefore might cause the fiber diameter to increase.[186,187]

LAES has many applications because in one step, a functional coating can be applied to the outer surface of fibers,[188] like a coating of silver nanoparticles can improve the performance of antimicrobial wound dressings[202] or water treatment membranes.[203] Hydrophilic PVP nanofibers have been coated with stearic acid to improve their moisture resistance for use in long-term storage applications.[204] As discussed in Section 4.1 "***Biomedical Applications***", a burst release effect can be avoided by fabricating core−sheath nanofibers containing drugs in the core using conventional coaxial electrospinning; however, that requires the sheath material to be spinnable. In contrast, LAES produced nanofibers can have nonspinnable sheaths encapsulating the drugs in the core, and this geometry will also mitigate a burst release.[205,206] One example of this is when Yu et al.[205] used a mixture of a ketoprofen and zein protein as the core and a dilute zein solution as the sheath to obtain nanofibers with a thin coating of zein, which showed a linear drug release profile without any burst release effect.[205]

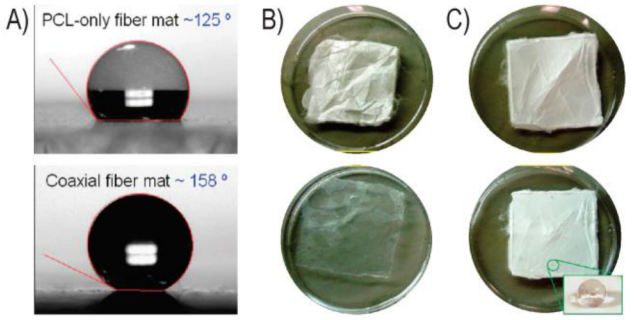

Figure 14. (A) A Teflon AF sheath enabled a fiber mat with a 158° superhydrophobic contact angle, whereas the PCL-only fiber mat had a water contact angle of 125°. (B) The gelatin-only fiber mat hydrated upon immersion in water, whereas (C) the fibers comprised of a gelatin core and a Teflon AF sheath did not absorb water. Figures 14A−C are reproduced with permission from ref 210. Copyright American Chemical Society 2009.

Nonspinnable or hard-to-spin precursors, such as Teflon, zein, and chitosan, can be processed as the sheath material using coaxial spinning featuring spinnable precursors as the core. Chitosan is a biodegradable and biocompatible polymer that is of particular interest due to its antimicrobial properties.[207] However, chitosan is difficult to electrospin in aqueous solutions due to its high viscosity at low polymer concentrations.[207] Nguyen et al.[208] obtained chitosan fibers from a 4 wt % precursor solution by using PLA as the core and observed that these core−sheath nanofibers completely inhibited the growth of *Escherichia coli* (*E. coli*) for 12 h.

https://dx.doi.org/10.1021/acsami.0c17706
ACS Appl. Mater. Interfaces 2021, 13, 48−66

Similarly, when Kalwar et al.[209] used PCL as a core layer and chitosan/silver nanoparticles as the sheath, the fibers had strong antibacterial properties against *E. coli* and *Staphylococcus aureus*.

Superhydrophobic fibers that have a water contact angle greater than 150° are important for many industrial textile applications due to their self-cleaning properties.[210] While Teflon fabrics could provide superhydrophobicity, the amorphous fluoropolymer (Teflon AF) is not electrospinnable due to its low dielectric constant that prevents the induction of sufficient charges. Han and Steckl,[210] as well as Muthiah et al.,[211] were able to obtain superhydrophobic mats via coaxial electrospinning by using Teflon AF as the sheath and PCL and PVDF, respectively, as the core, see Figure 14A. Han and Steckl[210] also obtained gelatin fibers coated with Teflon AF and compared their water uptake with gelatin-only fiber mats. While the gelatin-only fiber mat hydrated upon the immersion in water (Figure 14B), Teflon coated gelatin fiber mats did not absorb water (Figure 14C).

7. PERSPECTIVE

While the first published study on coaxial electrospinning emerged less than two decades ago, the process has proved to be a milestone for nanofiber fabrication. Because coaxial electrospinning can uniquely manufacture nanofibers from precursors that are typically considered "nonspinnable", the process can help society to fully realize the full potential of applications that nanoscale fibers have to offer. It provides a straightforward method to fabricate hollow fibers and/or encapsulate functional agents, including drugs, self-healing agents, and nanoparticles into robust fabrics. When coaxial electrospinning is used for drug encapsulation, the resulting fibers show a prolonged release profile, which is more desirable than the burst release typically achieved by simply mixing a drug and single-nozzle electrospinning. Self-healing agents encapsulated within coaxially electrospun fibers provide an on-demand release of healing agents that extend the lifetime of structural materials and protect surfaces from corrosion. Coaxial electrospinning can be used to encapsulate conductive materials, such as carbon nanotubes, inside an insulating polymer to advance nano- and microelectronics. Porous hollow fibers have been generated with improved catalytic activities because of their high surface area. However, to further understand the properties of porous fibers, a relationship between the parameters of coaxial electrospinning and the properties of the porous surface, such as the size distribution and number of pores, should be realized. When a triaxial or higher-order spinneret is used, multilayered and multifunctional fibers can be obtained, and thus, their applications are limitless.

Due to the applications of fibers in drug delivery, energy storage, and other advanced fields, coaxial electrospinning has been studied to a great extent at laboratory scale, and most studies have obtained random depositions of fibers. However, the full application potential of coaxial electrospinning can only be realized when their large-scale production is commercially viable. Additionally, many applications, including tissue engineering and separation membranes, would benefit from a scalable way to manufacture aligned or grids coaxial fibers with controllable interfiber spacings.

Coaxial electrospinning has been used to obtain polymeric and ceramic nanofibers. Unfortunately, metallic nanofibers, even though they have vast applications, have not yet been coaxially electrospun. In terms of polymers, many have limited or no solubility in solvents, thus they must be processed from the melt form, which has its own challenges. Of note is that when a polymer does have solubility, the solvents are often chosen based on their physical properties, such as volatility, conductivity, and surface tension. Unfortunately, oftentimes the spinning process is facilitated by using a "less-than-ideal" solvent, which may lack biocompatibility or environmental friendliness. For example, even though dimethylformamide and tetrahydrofuran are good solvents for many polymers and ideal for electrospinning, these toxic solvents inhibit the uses of the electrospun fibers. Moreover, we must move toward using green chemistry processes that ideally eliminate the generation of hazardous substances whenever possible. Having a better understanding of how polymer, solvent, and environmental parameters impact coaxially electrospun fibers holds the key to improving their large-scale production and implementation across applications. Imaginative, earth-conscious engineers might look toward modified coaxial setups to enable the production of nanotextiles from recycled polymers without relying on toxic solvents. We look forward to learning what complex nanofiber geometries and chemistries the next two decades of coaxial electrospinning will yield.

AUTHOR INFORMATION

Corresponding Author

Jessica D. Schiffman − *Department of Chemical Engineering, University of Massachusetts Amherst, Amherst, Massachusetts 01003-9303, United States;* orcid.org/0000-0002-1265-5392; Email: schiffman@ecs.umass.edu

Author

Prerana Rathore − *Department of Chemical Engineering, University of Massachusetts Amherst, Amherst, Massachusetts 01003-9303, United States;* orcid.org/0000-0002-9797-9766

Complete contact information is available at: https://pubs.acs.org/10.1021/acsami.0c17706

Notes

The authors declare no competing financial interest.

ACKNOWLEDGMENTS

The authors acknowledge the support from the National Science Foundation (Award #1921839).

REFERENCES

(1) Wang, B.; Wang, Y.; Yin, T.; Yu, Q. Applications of Electrospinning Technique in Drug Delivery. *Chem. Eng. Commun.* **2010**, *197*, 1315−1338.

(2) Ashammakhi, N.; Wimpenny, I.; Nikkola, L.; Yang, Y. Electrospinning: Methods and Development of Biodegradable Nanofibres for Drug Release. *J. Biomed. Nanotechnol.* **2009**, *5*, 1−19.

(3) Martins, A.; Reis, R. L.; Neves, N. M. Electrospinning: Processing Technique for Tissue Engineering Scaffolding. *Int. Mater. Rev.* **2008**, *53*, 257−274.

(4) Kanani, G. A.; Bahrami, H. S. Review on Electrospun Nanofibers Scaffold and Biomedical Applications. *Trends Biomater. Artif. Organs* **2010**, *24*, 93−115.

(5) Mercante, L. A.; Scagion, V. P.; Migliorini, F. L.; Mattoso, L. H. C.; Correa, D. S. Electrospinning-Based (Bio)Sensors for Food and Agricultural Applications: A Review. *TrAC, Trends Anal. Chem.* **2017**, *91*, 91−103.

https://dx.doi.org/10.1021/acsami.0c17706
ACS Appl. Mater. Interfaces 2021, 13, 48−66

(6) Sun, G.; Sun, L.; Xie, H.; Liu, J. Electrospinning of Nanofibers for Energy Applications. *Nanomaterials* **2016**, *6*, 129.
(7) Li, X.; Chen, Y.; Huang, H.; Mai, Y. W.; Zhou, L. Electrospun Carbon-Based Nanostructured Electrodes for Advanced Energy Storage - A Review. *Energy Storage Mater.* **2016**, *5*, 58−92.
(8) Eykens, L.; De Sitter, K.; Dotremont, C.; Pinoy, L.; Van der Bruggen, B. Membrane Synthesis for Membrane Distillation: A Review. *Sep. Purif. Technol.* **2017**, *182*, 36−51.
(9) Tijing, L. D.; Choi, J. S.; Lee, S.; Kim, S. H.; Shon, H. K. Recent Progress of Membrane Distillation Using Electrospun Nanofibrous Membrane. *J. Membr. Sci.* **2014**, *453*, 435−462.
(10) Pan, L.; Qiu, H.; Dou, C.; Li, Y.; Pu, L.; Xu, J.; Shi, Y. Conducting Polymer Nanostructures: Template Synthesis and Applications in Energy Storage. *Int. J. Mol. Sci.* **2010**, *11*, 2636−2657.
(11) Tao, S. L.; Desai, T. A. Aligned Arrays of Biodegradable Poly(ε-Caprolactone) Nanowires and Nanofibers by Template Synthesis. *Nano Lett.* **2007**, *7*, 1463−1468.
(12) Bajakova, J.; Chaloupek, J.; Lukaš, D.; Lacarin, M. "Drawing"-The Production of Individual Nanofibers by Experimental Method. In *NANOCON 2011 - Conference Proceedings, 3rd International Conference*; 2011; pp 322−326.
(13) Nain, A. S.; Wong, J. C.; Amon, C.; Sitti, M. Drawing Suspended Polymer Micro-/Nanofibers Using Glass Micropipettes. *Appl. Phys. Lett.* **2006**, *89*, 183105.
(14) Mille, M.; Lamère, J. F.; Rodrigues, F.; Fery-Forgues, S. Spontaneous Formation of Fluorescent Nanofibers from Self-Assembly of Low-Molecular-Weight Coumarin Derivatives in Water. *Langmuir* **2008**, *24*, 2671−2679.
(15) Pal, J.; Sanwaria, S.; Srivastava, R.; Nandan, B.; Horechyy, A.; Stamm, M.; Chen, H. L. Hairy Polymer Nanofibers via Self-Assembly of Block Copolymers. *J. Mater. Chem.* **2012**, *22*, 25102−25107.
(16) Shao, J.; Chen, C.; Wang, Y.; Chen, X.; Du, C. Early Stage Evolution of Structure and Nanoscale Property of Nanofibers in Thermally Induced Phase Separation Process. *React. Funct. Polym.* **2012**, *72*, 765−772.
(17) Zhao, J.; Han, W.; Chen, H.; Tu, M.; Zeng, R.; Shi, Y.; Cha, Z.; Zhou, C. Preparation, Structure and Crystallinity of Chitosan Nano-Fibers by a Solid-Liquid Phase Separation Technique. *Carbohydr. Polym.* **2011**, *83*, 1541−1546.
(18) Engström, J.; Hagström, B. Centrifugal Spinning of Nanofiber Webs: A Parameter Study of a Novel Spinning Process. *Nord. Text. J.* **2009**, *8*, 83.
(19) Weitz, R. T.; Harnau, L.; Rauschenbach, S.; Burghard, M.; Kern, K. Polymer Nanofibers via Nozzle-Free Centrifugal Spinning. *Nano Lett.* **2008**, *8*, 1187−1191.
(20) Reneker, D. H.; Yarin, A. L. Electrospinning Jets and Polymer Nanofibers. *Polymer* **2008**, *49*, 2387−2425.
(21) Loscertales, I. G.; Barrero, A.; Guerrero, I.; Cortijo, R.; Marquez, M.; Gañán-Calvo, A. M. Micro/Nano Encapsulation via Electrified Coaxial Liquid Jets. *Science* **2002**, *295*, 1695−1698.
(22) Sun, Z.; Zussman, E.; Yarin, A. L.; Wendorff, J. H.; Greiner, A. Compound Core-Shell Polymer Nanofibers by Co-Electrospinning. *Adv. Mater.* **2003**, *15*, 1929−1932.
(23) Zhang, Y.; Huang, Z. M.; Xu, X.; Lim, C. T.; Ramakrishna, S. Preparation of Core-Shell Structured PCL-r-Gelatin Bi-Component Nanofibers by Coaxial Electrospinning. *Chem. Mater.* **2004**, *16*, 3406−3409.
(24) Han, X. J.; Huang, Z.; He, C.; Liu, L. Preparation and Characterization of Core-Shell Structured Nanofibers by Coaxial Electrospinning. *High Perform. Polym.* **2007**, *19*, 147−159.
(25) Li, D.; Xia, Y. Direct Fabrication of Composite and Ceramic Hollow Nanofibers by Electrospinning. *Nano Lett.* **2004**, *4*, 933−938.
(26) Loscertales, I. G.; Barrero, A.; Márquez, M.; Spretz, R.; Velarde-Ortiz, R.; Larsen, G. Electrically Forced Coaxial Nanojets for One-Step Hollow Nanofiber Design. *J. Am. Chem. Soc.* **2004**, *126*, 5376−5377.
(27) Han, D.; Steckl, A. J. Coaxial Electrospinning Formation of Complex Polymer Fibers and Their Applications. *ChemPlusChem* **2019**, *84*, 1453−1497.
(28) Qu, H.; Wei, S.; Guo, Z. Coaxial Electrospun Nanostructures and Their Applications. *J. Mater. Chem. A* **2013**, *1*, 11513−11528.
(29) Sundarrajan, S.; Murugan, R.; Nair, A. S.; Ramakrishna, S. Fabrication of P3HT/PCBM Solar Cloth by Electrospinning Technique. *Mater. Lett.* **2010**, *64*, 2369−2372.
(30) Xue, R.; Behera, P.; Xu, J.; Viapiano, M. S.; Lannutti, J. J. Polydimethylsiloxane Core−Polycaprolactone Shell Nanofibers as Biocompatible, Real-Time Oxygen Sensors. *Sens. Actuators, B* **2014**, *192*, 697−707.
(31) Taylor, G. I. Disintegration of Water Drops in an Electric Field. *Proc. R. Soc. London Ser. Math. Phys. Sci.* **1964**, *280*, 383−397.
(32) Baumgarten, P. K. Electrostatic Spinning of Acrylic Microfibers. *J. Colloid Interface Sci.* **1971**, *36*, 71−79.
(33) Reneker, D. H.; Yarin, A. L.; Fong, H.; Koombhongse, S. Bending Instability of Electrically Charged Liquid Jets of Polymer Solutions in Electrospinning. *J. Appl. Phys.* **2000**, *87*, 4531−4547.
(34) Yarin, A. L.; Koombhongse, S.; Reneker, D. H. Taylor Cone and Jetting from Liquid Droplets in Electrospinning of Nanofibers. *J. Appl. Phys.* **2001**, *90*, 4836−4846.
(35) Yarin, A. L.; Koombhongse, S.; Reneker, D. H. Bending Instability in Electrospinning of Nanofibers. *J. Appl. Phys.* **2001**, *89*, 3018−3026.
(36) Schiffman, J. D.; Schauer, C. L. A Review: Electrospinning of Biopolymer Nanofibers and Their Applications. *Polym. Rev.* **2008**, *48*, 317−352.
(37) Rutledge, G. C.; Fridrikh, S. V. Formation of Fibers by Electrospinning. *Adv. Drug Delivery Rev.* **2007**, *59*, 1384−1391.
(38) *Polymeric Nanofibers*; Reneker, D. H., Fong, H., Eds.; ACS Symposium Series; American Chemical Society: Washington, DC, 2006; Vol. *918*.
(39) Kaerkitcha, N.; Chuangchote, S.; Sagawa, T. Control of Physical Properties of Carbon Nanofibers Obtained from Coaxial Electrospinning of PMMA and PAN with Adjustable Inner/Outer Nozzle-Ends. *Nanoscale Res. Lett.* **2016**, *11*, 17−21.
(40) Reznik, S. N.; Yarin, A. L.; Zussman, E.; Bercovici, L. Evolution of a Compound Droplet Attached to a Core-Shell Nozzle under the Action of a Strong Electric Field. *Phys. Fluids* **2006**, *18*, No. 062101.
(41) Jiang, H.; Hu, Y.; Li, Y.; Zhao, P.; Zhu, K.; Chen, W. A Facile Technique to Prepare Biodegradable Coaxial Electrospun Nanofibers for Controlled Release of Bioactive Agents. *J. Controlled Release* **2005**, *108*, 237−243.
(42) Song, T.; Zhang, Y.; Zhou, T.; Lim, C. T.; Ramakrishna, S.; Liu, B. Encapsulation of Self-Assembled FePt Magnetic Nanoparticles in PCL Nanofibers by Coaxial Electrospinning. *Chem. Phys. Lett.* **2005**, *415*, 317−322.
(43) Zussman, E.; Yarin, A. L.; Bazilevsky, A. V.; Avrahami, R.; Feldman, M. Electrospun Polyacrylonitrile/Poly(Methyl Methacrylate)-Derived Turbostratic Carbon Micro-/Nanotubes. *Adv. Mater.* **2006**, *18*, 348−353.
(44) Yu, H. J.; Fridrikh, S. V.; Rutledge, G. C. Production of Submicrometer Diameter Fibers by Two-Fluid Electrospinnig. *Adv. Mater.* **2004**, *16*, 1562−1566.
(45) Wang, M.; Jing, N.; Su, C. B.; Kameoka, J.; Chou, C. K.; Hung, M. C.; Chang, K. A. Electrospinning of Silica Nanochannels for Single Molecule Detection. *Appl. Phys. Lett.* **2006**, *88*, No. 033106.
(46) Lee, B. S.; Jeon, S. Y.; Park, H.; Lee, G.; Yang, H. S.; Yu, W. R. New Electrospinning Nozzle to Reduce Jet Instability and Its Application to Manufacture of Multi-Layered Nanofibers. *Sci. Rep.* **2015**, *4*, 6758.
(47) Chen, H.; Wang, N.; Di, J.; Zhao, Y.; Song, Y.; Jiang, L. Nanowire-in-Microtube Structured Core/Shell Fibers via Multifluidic Coaxial Electrospinning. *Langmuir* **2010**, *26*, 11291−11296.
(48) Chen, Y.; Lu, Z.; Zhou, L.; Mai, Y. W.; Huang, H. Triple-Coaxial Electrospun Amorphous Carbon Nanotubes with Hollow Graphitic Carbon Nanospheres for High-Performance Li Ion Batteries. *Energy Environ. Sci.* **2012**, *5*, 7898−7902.
(49) Han, D.; Steckl, A. J. Triaxial Electrospun Nanofiber Membranes for Controlled Dual Release of Functional Molecules. *ACS Appl. Mater. Interfaces* **2013**, *5*, 8241−8245.

https://dx.doi.org/10.1021/acsami.0c17706
ACS Appl. Mater. Interfaces 2021, 13, 48−66

(50) Chen, J. Y.; Wu, H. C.; Chiu, Y. C.; Lin, C. J.; Tung, S. H.; Chen, W. C. Electrospun Poly(3-Hexylthiophene) Nanofibers with Highly Extended and Oriented Chains through Secondary Electric Field for High-Performance Field-Effect Transistors. *Adv. Electron. Mater.* **2015**, *1*, 1400028.
(51) Elahi, Md. F.; Lu, W. Core-Shell Fibers for Biomedical Applications-A Review. *J. Bioeng. Biomed. Sci.* **2013**, *03*, 1−14.
(52) Yoon, J.; Yang, H. S.; Lee, B. S.; Yu, W. R. Recent Progress in Coaxial Electrospinning: New Parameters, Various Structures, and Wide Applications. *Adv. Mater.* **2018**, *30*, 1704765.
(53) Demir, M. M.; Yilgor, I.; Yilgor, E.; Erman, B. Electrospinning of Polyurethane Fibers. *Polymer* **2002**, *43*, 3303−3309.
(54) Yao, Z. C.; Chen, S. C.; Ahmad, Z.; Huang, J.; Chang, M. W.; Li, J. S. Essential Oil Bioactive Fibrous Membranes Prepared via Coaxial Electrospinning. *J. Food Sci.* **2017**, *82*, 1412−1422.
(55) Zhang, J.; Choi, S. W.; Kim, S. S. Micro- and Nano-Scale Hollow TiO_2 Fibers by Coaxial Electrospinning: Preparation and Gas Sensing. *J. Solid State Chem.* **2011**, *184*, 3008−3013.
(56) He, C. L.; Huang, Z. M.; Han, X. J.; Liu, L.; Zhang, H. S.; Chen, L. S. Coaxial Electrospun Poly(L-Lactic Acid) Ultrafine Fibers for Sustained Drug Delivery. *J. Macromol. Sci., Part B: Phys.* **2006**, *45*, 515−524.
(57) Li, D.; Babel, A.; Jenekhe, S. A.; Xia, Y. Nanofibers of Conjugated Polymers Prepared by Electrospinning with a Two-Capillary Spinneret. *Adv. Mater.* **2004**, *16*, 2062−2066.
(58) Moghe, A. K.; Gupta, B. S. Co-Axial Electrospinning for Nanofiber Structures: Preparation and Applications. *Polym. Rev.* **2008**, *48*, 353−377.
(59) McCann, J. T.; Li, D.; Xia, Y. Electrospinning of Nanofibers with Core-Sheath, Hollow, or Porous Structures. *J. Mater. Chem.* **2005**, *15*, 735−738.
(60) Xin, Y.; Huang, Z.; Li, W.; Jiang, Z.; Tong, Y.; Wang, C. Core−Sheath Functional Polymer Nanofibers Prepared by Co-Electrospinning. *Eur. Polym. J.* **2008**, *44*, 1040−1045.
(61) Li, D.; McCann, J. T.; Xia, Y. Use of Electrospinning to Directly Fabricate Hollow Nanofibers with Functionalized Inner and Outer Surfaces. *Small* **2005**, *1*, 83−86.
(62) Anka, F. H.; Balkus, K. J. Novel Nanofiltration Hollow Fiber Membrane Produced via Electrospinning. *Ind. Eng. Chem. Res.* **2013**, *52*, 3473−3480.
(63) Chan, K. H. K.; Kotaki, M. Fabrication and Morphology Control of Poly(Methyl Methacrylate) Hollow Structures via Coaxial Electrospinning. *J. Appl. Polym. Sci.* **2009**, *111*, 408−416.
(64) Khalf, A.; Singarapu, K.; Madihally, S. V. Cellulose Acetate Core−Shell Structured Electrospun Fiber: Fabrication and Characterization. *Cellulose* **2015**, *22*, 1389−1400.
(65) Luo, C. J.; Edirisinghe, M. Core-Liquid-Induced Transition from Coaxial Electrospray to Electrospinning of Low-Viscosity Poly(Lactide- Co -Glycolide) Sheath Solution. *Macromolecules* **2014**, *47*, 7930−7938.
(66) Yao, Z. C.; Chang, M. W.; Ahmad, Z.; Li, J. S. Encapsulation of Rose Hip Seed Oil into Fibrous Zein Films for Ambient and on Demand Food Preservation via Coaxial Electrospinning. *J. Food Eng.* **2016**, *191*, 115−123.
(67) Raeesi, F.; Nouri, M.; Haghi, A. K. Electrospinning of Polyaniline-Polyacrylonitrile Blend Nanofibers. *e-Polym.* **2009**, *9*, 114.
(68) Larrondo, L.; Manley, R. S. J. Electrostatic Fiber Spinning from Polymer Melts - 1. Experimental Observations on Fiber Formation and Properties. *J. Polym. Sci., Polym. Phys. Ed.* **1981**, *19*, 909−920.
(69) Choi, J.; Lee, J.; Choi, J.; Jung, D.; Shim, S. E. Electrospun PEDOT:PSS/PVP Nanofibers as the Chemiresistor in Chemical Vapour Sensing. *Synth. Met.* **2010**, *160*, 1415−1421.
(70) Meechaisue, C.; Dubin, R.; Supaphol, P.; Hoven, V. P.; Kohn, J. Electrospun Mat of Tyrosine-Derived Polycarbonate Fibers for Potential Use as Tissue Scaffolding Material. *J. Biomater. Sci., Polym. Ed.* **2006**, *17*, 1039−1056.
(71) Haider, A.; Haider, S.; Kang, I. K. A Comprehensive Review Summarizing the Effect of Electrospinning Parameters and Potential Applications of Nanofibers in Biomedical and Biotechnology. *Arabian J. Chem.* **2018**, *11*, 1165−1188.
(72) Niu, H.; Wang, H.; Zhou, H.; Lin, T. Ultrafine PDMS Fibers: Preparation from in Situ Curing-Electrospinning and Mechanical Characterization. *RSC Adv.* **2014**, *4*, 11782−11787.
(73) Di, J.; Chen, H.; Wang, X.; Zhao, Y.; Jiang, L.; Yu, J.; Xu, R. Fabrication of Zeolite Hollow Fibers by Coaxial Electrospinning. *Chem. Mater.* **2008**, *20*, 3543−3545.
(74) He, M.; Jiang, H.; Wang, R.; Xie, Y.; Zhao, C. Fabrication of Metronidazole Loaded Poly (ε-Caprolactone)/Zein Core/Shell Nanofiber Membranes via Coaxial Electrospinning for Guided Tissue Regeneration. *J. Colloid Interface Sci.* **2017**, *490*, 270−278.
(75) Wang, M.; Yu, J. H.; Kaplan, D. L.; Rutledge, G. C. Production of Submicron Diameter Silk Fibers under Benign Processing Conditions by Two-Fluid Electrospinning. *Macromolecules* **2006**, *39*, 1102−1107.
(76) Zhang, Y. Z.; Wang, X.; Feng, Y.; Li, J.; Lim, C. T.; Ramakrishna, S. Coaxial Electrospinning of (Fluorescein Isothiocyanate-Conjugated Bovine Serum Albumin)-Encapsulated Poly(ε-Caprolactone) Nanofibers for Sustained Release. *Biomacromolecules* **2006**, *7*, 1049−1057.
(77) Song, T.; Zhang, Y. Z.; Zhou, T. J. Fabrication of Magnetic Composite Nanofibers of Poly(ε-Caprolactone) with FePt Nanoparticles by Coaxial Electrospinning. *J. Magn. Magn. Mater.* **2006**, *303*, e286−e289.
(78) Chang, W.; Xu, F.; Mu, X.; Ji, L.; Ma, G.; Nie, J. Fabrication of Nanostructured Hollow TiO_2 Nanofibers with Enhanced Photocatalytic Activity by Coaxial Electrospinning. *Mater. Res. Bull.* **2013**, *48*, 2661−2668.
(79) Chang, G. Q.; Zheng, X.; Chen, R. Y.; Chen, X.; Chen, L. Q.; Chen, Z. Silver Nanoparticles Filling in TiO_2 Hollow Nanofibers by Coaxial Electrospinning. *Acta Phys. - Chim. Sin.* **2008**, *24*, 1790−1797.
(80) Cao, J.; Dou, H.; Zhang, H.; Mei, H.; Liu, S.; Fei, T.; Wang, R.; Wang, L.; Zhang, T. Controllable Synthesis and HCHO-Sensing Properties of In_2O_3 Micro/Nanotubes with Different Diameters. *Sens. Actuators, B* **2014**, *198*, 180−187.
(81) Choi, S. J.; Chattopadhyay, S.; Kim, J. J.; Kim, S. J.; Tuller, H. L.; Rutledge, G. C.; Kim, I. D. Coaxial Electrospinning of WO_3 Nanotubes Functionalized with Bio-Inspired Pd Catalysts and Their Superior Hydrogen Sensing Performance. *Nanoscale* **2016**, *8*, 9159−9166.
(82) Cao, J.; Zhang, T.; Li, F.; Yang, H.; Liu, S. Enhanced Ethanol Sensing of SnO_2 Hollow Micro/Nanofibers Fabricated by Coaxial Electrospinning. *New J. Chem.* **2013**, *37*, 2031−2036.
(83) Liu, S.; Yu, B.; Li, F.; Ji, Y.; Zhang, T. Coaxial Electrospinning Route to Prepare Au-Loading SnO_2 Hollow Microtubes for Non-Enzymatic Detection of H_2O_2. *Electrochim. Acta* **2014**, *141*, 161−166.
(84) Bagheri, H.; Rezvani, O.; Banihashemi, S. Core-Shell Electrospun Polybutylene Terephthalate/Polypyrrole Hollow Nanofibers for Micro-Solid Phase Extraction. *J. Chromatogr. A* **2016**, *1434*, 19−28.
(85) Halaui, R.; Moldavsky, A.; Cohen, Y.; Semiat, R.; Zussman, E. Development of Micro-Scale Hollow Fiber Ultrafiltration Membranes. *J. Membr. Sci.* **2011**, *379*, 370−377.
(86) Halaui, R.; Zussman, E.; Khalfin, R.; Semiat, R.; Cohen, Y. Polymeric Microtubes for Water Filtration by Co-Axial Electrospinning Technique. *Polym. Adv. Technol.* **2017**, *28*, 570−582.
(87) Lee, B.-S.; Park, K.-M.; Yu, W.-R.; Youk, J. H. An Effective Method for Manufacturing Hollow Carbon Nanofibers and Microstructural Analysis. *Macromol. Res.* **2012**, *20*, 605−613.
(88) Lee, B. S.; Son, S. B.; Park, K. M.; Lee, G.; Oh, K. H.; Lee, S. H.; Yu, W. R. Effect of Pores in Hollow Carbon Nanofibers on Their Negative Electrode Properties for a Lithium Rechargeable Battery. *ACS Appl. Mater. Interfaces* **2012**, *4*, 6702−6710.
(89) Lee, B. S.; Son, S. B.; Park, K. M.; Yu, W. R.; Oh, K. H.; Lee, S. H. Anodic Properties of Hollow Carbon Nanofibers for Li-Ion Battery. *J. Power Sources* **2012**, *199*, 53−60.
(90) Wang, X.; Li, Y.; Jin, T.; Meng, J.; Jiao, L.; Zhu, M.; Chen, J. Electrospun Thin-Walled $CuCo_2O_4$@C Nanotubes as Bifunctional

https://dx.doi.org/10.1021/acsami.0c17706
ACS Appl. Mater. Interfaces 2021, 13, 48−66

Oxygen Electrocatalysts for Rechargeable Zn-Air Batteries. *Nano Lett.* **2017**, *17*, 7989−7994.
(91) Wu, Y.; Gao, M.; Li, X.; Liu, Y.; Pan, H. Preparation of Mesohollow and Microporous Carbon Nanofiber and Its Application in Cathode Material for Lithium-Sulfur Batteries. *J. Alloys Compd.* **2014**, *608*, 220−228.
(92) Jia, X.; Zhao, C.; Li, P.; Zhang, H.; Huang, Y.; Li, H.; Fan, J.; Feng, W.; Yuan, X.; Fan, Y. Sustained Release of VEGF by Coaxial Electrospun Dextran/PLGA Fibrous Membranes in Vascular Tissue Engineering. *J. Biomater. Sci., Polym. Ed.* **2011**, *22*, 1811−1827.
(93) Ou, K. L.; Chen, C. S.; Lin, L. H.; Lu, J. C.; Shu, Y. C.; Tseng, W. C.; Yang, J. C.; Lee, S. Y.; Chen, C. C. Membranes of Epitaxial-like Packed, Super Aligned Electrospun Micron Hollow Poly(L-Lactic Acid) (PLLA) Fibers. *Eur. Polym. J.* **2011**, *47*, 882−892.
(94) Wang, B.; Zheng, H.; Chang, M. W.; Ahmad, Z.; Li, J. S. Hollow Polycaprolactone Composite Fibers for Controlled Magnetic Responsive Antifungal Drug Release. *Colloids Surf., B* **2016**, *145*, 757−767.
(95) Hou, H.; Jun, Z.; Reuning, A.; Schaper, A.; Wendorff, J. H.; Greiner, A. Poly(p-Xylylene) Nanotubes by Coating and Removal of Ultrathin Polymer Template Fibers. *Macromolecules* **2002**, *35*, 2429−2431.
(96) Dersch, R.; Steinhart, M.; Boudriot, U.; Greiner, A.; Wendorff, J. H. Nanoprocessing of Polymers: Applications in Medicine, Sensors, Catalysis, Photonics. *Polym. Adv. Technol.* **2005**, *16*, 276−282.
(97) Wei, Z.; Zhang, Z.; Wan, M. Formation Mechanism of Self-Assembled Polyaniline Micro/Nanotubes. *Langmuir* **2002**, *18*, 917−921.
(98) Wan, M.; Wei, Z.; Zhang, Z.; Zhang, L.; Huang, K.; Yang, Y. Studies on Nanostructures of Conducting Polymers via Self-Assembly Method. *Synth. Met.* **2003**, *135*−*136*, 175−176.
(99) Su, C.; Li, Y.; Cao, H.; Lu, C.; Li, Y.; Chang, J.; Duan, F. Novel PTFE Hollow Fiber Membrane Fabricated by Emulsion Electrospinning and Sintering for Membrane Distillation. *J. Membr. Sci.* **2019**, *583*, 200−208.
(100) Zeng, W.; Chen, W.; Li, Z.; Zhang, H.; Li, T. Rapid and Sensitive Ethanol Sensor Based on Hollow Au/V_2O_5 Nanotubes via Emulsion-Electrospinning Route. *Mater. Res. Bull.* **2015**, *65*, 157−162.
(101) Lee, G. H.; Song, J. C.; Yoon, K. B. Controlled Wall Thickness and Porosity of Polymeric Hollow Nanofibers by Coaxial Electrospinning. *Macromol. Res.* **2010**, *18*, 571−576.
(102) Díaz, J. E.; Fernández-Nieves, A.; Barrero, A.; Márquez, M.; Loscertales, I. G. Fabrication of Structured Micro and Nanofibers by Coaxial Electrospinning. *J. Phys. Conf. Ser.* **2008**, *127*, No. 012008.
(103) Pakravan, M.; Heuzey, M. C.; Ajji, A. Core-Shell Structured PEO-Chitosan Nanofibers by Coaxial Electrospinning. *Biomacromolecules* **2012**, *13*, 412−421.
(104) Rajala, J. W.; Shin, H. U.; Lolla, D.; Chase, G. G. Core−Shell Electrospun Hollow Aluminum Oxide Ceramic Fibers. *Fibers* **2015**, *3*, 450−462.
(105) Yuan, T.; Zhao, B.; Cai, R.; Zhou, Y.; Shao, Z. Electrospinning Based Fabrication and Performance Improvement of Film Electrodes for Lithium-Ion Batteries Composed of TiO_2 Hollow Fibers. *J. Mater. Chem.* **2011**, *21*, 15041−15048.
(106) Fu, Q.; Hou, J.; Lu, R.; Lin, C.; Ma, Y.; Li, J.; Chen, Y. Electrospun $Ti_2Nb_{10}O_{29}$ Hollow Nanofibers as High-Performance Anode Materials for Lithium-Ion Batteries. *Mater. Lett.* **2018**, *214*, 60−63.
(107) Cui, Z.; Wang, S.; Zhang, Y.; Cao, M. High-Performance Lithium Storage of Co_3O_4 Achieved by Constructing Porous Nanotube Structure. *Electrochim. Acta* **2015**, *182*, 507−515.
(108) Zhang, X.; Thavasi, V.; Mhaisalkar, S. G.; Ramakrishna, S. Novel Hollow Mesoporous 1D TiO_2 Nanofibers as Photovoltaic and Photocatalytic Materials. *Nanoscale* **2012**, *4*, 1707−1716.
(109) Zhang, X.; Aravindan, V.; Kumar, P. S.; Liu, H.; Sundaramurthy, J.; Ramakrishna, S.; Madhavi, S. Synthesis of TiO_2 Hollow Nanofibers by Co-Axial Electrospinning and Its Superior Lithium Storage Capability in Full-Cell Assembly with Olivine Phosphate. *Nanoscale* **2013**, *5*, 5973−5980.
(110) Yu, S.; Kim, J.; Yoon, K. R.; Jung, J. W.; Oh, J.; Kim, I. D. Rational Design of Efficient Electrocatalysts for Hydrogen Evolution Reaction: Single Layers of WS_2 Nanoplates Anchored to Hollow Nitrogen-Doped Carbon Nanofibers. *ACS Appl. Mater. Interfaces* **2015**, *7*, 28116−28121.
(111) Ji, X.; Su, Z.; Wang, P.; Ma, G.; Zhang, S. Polyelectrolyte Doped Hollow Nanofibers for Positional Assembly of Bienzyme System for Cascade Reaction at O/W Interface. *ACS Catal.* **2014**, *4*, 4548−4559.
(112) Dror, Y.; Salalha, W.; Avrahami, R.; Zussman, E.; Yarin, A. L.; Dersch, R.; Greiner, A.; Wendorff, J. H. One-Step Production of Polymeric Microtubes by Co-Electrospinning. *Small* **2007**, *3*, 1064−1073.
(113) Na, H.; Chen, P.; Wong, S. C.; Hague, S.; Li, Q. Fabrication of PVDF/PVA Microtubules by Coaxial Electrospinning. *Polymer* **2012**, *53*, 2736−2743.
(114) Asli, M. M.; Pourdeyhimi, B.; Loboa, E. G. Release Profiles of Tricalcium Phosphate Nanoparticles from Poly(L-Lactic Acid) Electrospun Scaffolds with Single Component, Core-Sheath, or Porous Fiber Morphologies: Effects on HASC Viability and Osteogenic Differentiation. *Macromol. Biosci.* **2012**, *12*, 893−900.
(115) He, P.; Zhong, Q.; Ge, Y.; Guo, Z.; Tian, J.; Zhou, Y.; Ding, S.; Li, H.; Zhou, C. Dual Drug Loaded Coaxial Electrospun PLGA/PVP Fiber for Guided Tissue Regeneration under Control of Infection. *Mater. Sci. Eng., C* **2018**, *90*, 549−556.
(116) Illangakoon, U. E.; Yu, D.-G.; Ahmad, B. S.; Chatterton, N. P.; Williams, G. R. 5-Fluorouracil Loaded Eudragit Fibers Prepared by Electrospinning. *Int. J. Pharm.* **2015**, *495*, 895−902.
(117) Park, J. H.; Braun, P. V. Coaxial Electrospinning of Self-Healing Coatings. *Adv. Mater.* **2010**, *22*, 496−499.
(118) Mitchell, T. J.; Keller, M. W. Coaxial Electrospun Encapsulation of Epoxy for Use in Self-Healing Materials. *Polym. Int.* **2013**, *62*, 860−866.
(119) An, S.; Liou, M.; Song, K. Y.; Jo, H. S.; Lee, M. W.; Al-Deyab, S. S.; Yarin, A. L.; Yoon, S. S. Highly Flexible Transparent Self-Healing Composite Based on Electrospun Core-Shell Nanofibers Produced by Coaxial Electrospinning for Anti-Corrosion and Electrical Insulation. *Nanoscale* **2015**, *7*, 17778−17785.
(120) Neisiany, R. E.; Khorasani, S. N.; Lee, J. K. Y.; Ramakrishna, S. Encapsulation of Epoxy and Amine Curing Agent in PAN Nanofibres by Coaxial Electrospinning for Self-Healing Purposes. *RSC Adv.* **2016**, *6*, 70056−70063.
(121) Lee, M. W.; An, S.; Kim, Y. I.; Yoon, S. S.; Yarin, A. L. Self-Healing Three-Dimensional Bulk Materials Based on Core-Shell Nanofibers. *Chem. Eng. J.* **2018**, *334*, 1093−1100.
(122) McCann, J. T.; Marquez, M.; Xia, Y. Melt Coaxial Electrospinning: A Versatile Method for the Encapsulation of Solid Materials and Fabrication of Phase Change Nanofibers. *Nano Lett.* **2006**, *6*, 2868−2872.
(123) Hu, W.; Yu, X. Encapsulation of Bio-Based PCM with Coaxial Electrospun Ultrafine Fibers. *RSC Adv.* **2012**, *2*, 5580−5584.
(124) Van Do, C.; Nguyen, T. T. T.; Park, J. S. Fabrication of Polyethylene Glycol/Polyvinylidene Fluoride Core/Shell Nanofibers via Melt Electrospinning and Their Characteristics. *Sol. Energy Mater. Sol. Cells* **2012**, *104*, 131−139.
(125) Sun, S. X.; Xie, R.; Wang, X. X.; Wen, G. Q.; Liu, Z.; Wang, W.; Ju, X. J.; Chu, L. Y. Fabrication of Nanofibers with Phase-Change Core and Hydrophobic Shell, via Coaxial Electrospinning Using Nontoxic Solvent. *J. Mater. Sci.* **2015**, *50*, 5729−5738.
(126) Rezaei, B.; Ghani, M.; Askari, M.; Shoushtari, A. M.; Malek, R. M. A. Fabrication of Thermal Intelligent Core/Shell Nanofibers by the Solution Coaxial Electrospinning Process. *Adv. Polym. Technol.* **2016**, *35*, 1−8.
(127) Lu, Y.; Xiao, X.; Fu, J.; Huan, C.; Qi, S.; Zhan, Y.; Zhu, Y.; Xu, G. Novel Smart Textile with Phase Change Materials Encapsulated Core-Sheath Structure Fabricated by Coaxial Electrospinning. *Chem. Eng. J.* **2019**, *355*, 532−539.

https://dx.doi.org/10.1021/acsami.0c17706
ACS Appl. Mater. Interfaces 2021, 13, 48−66

(128) Hwang, T. H.; Lee, Y. M.; Kong, B.-S.; Seo, J.-S.; Choi, J. W. Electrospun Core−Shell Fibers for Robust Silicon Nanoparticle-Based Lithium Ion Battery Anodes. *Nano Lett.* **2012**, *12*, 802−807.
(129) Enz, E.; Baumeister, U.; Lagerwall, J. Coaxial Electrospinning of Liquid Crystal-Containing Poly(Vinylpyrrolidone) Microfibres. *Beilstein J. Org. Chem.* **2009**, *5*, 58.
(130) Lagerwall, J. P. F.; McCann, J. T.; Formo, E.; Scalia, G.; Xia, Y. Coaxial Electrospinning of Microfibres with Liquid Crystal in the Core. *Chem. Commun.* **2008**, 5420−5422.
(131) Pant, B.; Park, M.; Park, S. J. Drug Delivery Applications of Core-Sheath Nanofibers Prepared by Coaxial Electrospinning: A Review. *Pharmaceutics* **2019**, *11*, 305−305.
(132) McClellan, P.; Landis, W. J. Recent Applications of Coaxial and Emulsion Electrospinning Methods in the Field of Tissue Engineering. *BioRes. Open Access* **2016**, *5*, 212−227.
(133) Lu, Y.; Huang, J.; Yu, G.; Cardenas, R.; Wei, S.; Wujcik, E. K.; Guo, Z. Coaxial Electrospun Fibers: Applications in Drug Delivery and Tissue Engineering. *Wiley Interdiscip. Rev. Nanomed. Nanobiotechnol.* **2016**, *8*, 654−677.
(134) Khalf, A.; Madihally, S. V. Recent Advances in Multiaxial Electrospinning for Drug Delivery. *Eur. J. Pharm. Biopharm.* **2017**, *112*, 1−17.
(135) Hu, W.; Huang, Z.-M.; Liu, X.-Y. Development of Braided Drug-Loaded Nanofiber Sutures. *Nanotechnology* **2010**, *21*, 315104.
(136) Choi, J. S.; Choi, S. H.; Yoo, H. S. Coaxial Electrospun Nanofibers for Treatment of Diabetic Ulcers with Binary Release of Multiple Growth Factors. *J. Mater. Chem.* **2011**, *21*, 5258−5267.
(137) He, M.; Xue, J.; Geng, H.; Gu, H.; Chen, D.; Shi, R.; Zhang, L. Fibrous Guided Tissue Regeneration Membrane Loaded with Anti-Inflammatory Agent Prepared by Coaxial Electrospinning for the Purpose of Controlled Release. *Appl. Surf. Sci.* **2015**, *335*, 121−129.
(138) Jin, G.; Prabhakaran, M. P.; Kai, D.; Ramakrishna, S. Controlled Release of Multiple Epidermal Induction Factors through Core−Shell Nanofibers for Skin Regeneration. *Eur. J. Pharm. Biopharm.* **2013**, *85*, 689−698.
(139) Kalani, M. M.; Nourmohammadi, J.; Negahdari, B.; Rahimi, A.; Sell, S. A. Electrospun Core-Sheath Poly(Vinyl Alcohol)/Silk Fibroin Nanofibers with Rosuvastatin Release Functionality for Enhancing Osteogenesis of Human Adipose-Derived Stem Cells. *Mater. Sci. Eng., C* **2019**, *99*, 129−139.
(140) Kiatyongchai, T.; Wongsasulak, S.; Yoovidhya, T. Coaxial Electrospinning and Release Characteristics of Cellulose Acetate-Gelatin Blend Encapsulating a Model Drug. *J. Appl. Polym. Sci.* **2014**, *131*, 40167.
(141) Liao, I. C.; Chew, S. Y.; Leong, K. W. Aligned Core-Shell Nanofibers Delivering Bioactive Proteins. *Nanomedicine* **2006**, *1*, 465−471.
(142) Repanas, A.; Glasmacher, B. Dipyridamole Embedded in Polycaprolactone Fibers Prepared by Coaxial Electrospinning as a Novel Drug Delivery System. *J. Drug Delivery Sci. Technol.* **2015**, *29*, 132−142.
(143) Rubert, M.; Dehli, J.; Li, Y.-F.; Taskin, M. B.; Xu, R.; Besenbacher, F.; Chen, M. Electrospun PCL/PEO Coaxial Fibers for Basic Fibroblast Growth Factor Delivery. *J. Mater. Chem. B* **2014**, *2*, 8538−8546.
(144) Saraf, A.; Baggett, L. S.; Raphael, R. M.; Kasper, F. K.; Mikos, A. G. Regulated Non-Viral Gene Delivery from Coaxial Electrospun Fiber Mesh Scaffolds. *J. Controlled Release* **2010**, *143*, 95−103.
(145) Sohrabi, A.; Shaibani, P. M.; Etayash, H.; Kaur, K.; Thundat, T. Sustained Drug Release and Antibacterial Activity of Ampicillin Incorporated Poly(Methyl Methacrylate)−Nylon6 Core/Shell Nanofibers. *Polymer* **2013**, *54*, 2699−2705.
(146) Wang, C. Y.; Liu, J. J.; Fan, C. Y.; Mo, X. M.; Ruan, H. J.; Li, F. F. The Effect of Aligned Core-Shell Nanofibres Delivering NGF on the Promotion of Sciatic Nerve Regeneration. *J. Biomater. Sci., Polym. Ed.* **2012**, *23*, 167−184.
(147) Wei, Q.; Xu, F.; Xu, X.; Geng, X.; Ye, L.; Zhang, A.; Feng, Z. The Multifunctional Wound Dressing with Core−Shell Structured Fibers Prepared by Coaxial Electrospinning. *Front. Mater. Sci.* **2016**, *10*, 113−121.
(148) Wen, S.; Hu, Y.; Zhang, Y.; Huang, S.; Zuo, Y.; Min, Y. Dual-Functional Core-Shell Electrospun Mats with Precisely Controlled Release of Anti-Inflammatory and Anti-Bacterial Agents. *Mater. Sci. Eng., C* **2019**, *100*, 514−522.
(149) Yu, H.; Yang, P.; Jia, Y.; Zhang, Y.; Ye, Q.; Zeng, S. Regulation of Biphasic Drug Release Behavior by Graphene Oxide in Polyvinyl Pyrrolidone/Poly(ε-Caprolactone) Core/Sheath Nanofiber Mats. *Colloids Surf., B* **2016**, *146*, 63−69.
(150) Ball, C.; Chou, S.-F.; Jiang, Y.; Woodrow, K. A. Coaxially Electrospun Fiber-Based Microbicides Facilitate Broadly Tunable Release of Maraviroc. *Mater. Sci. Eng., C* **2016**, *63*, 117−124.
(151) He, C. L.; Huang, Z. M.; Han, X. J. Fabrication of Drug-Loaded Electrospun Aligned Fibrous Threads for Suture Applications. *J. Biomed. Mater. Res., Part A* **2009**, *89A*, 80−95.
(152) Huang, Z.-M.; He, C.-L.; Yang, A.; Zhang, Y.; Han, X.-J.; Yin, J.; Wu, Q. Encapsulating Drugs in Biodegradable Ultrafine Fibers through Co-Axial Electrospinning. *J. Biomed. Mater. Res., Part A* **2006**, *77A*, 169−179.
(153) Ji, W.; Yang, F.; Van Den Beucken, J. J. J. P.; Bian, Z.; Fan, M.; Chen, Z.; Jansen, J. A. Fibrous Scaffolds Loaded with Protein Prepared by Blend or Coaxial Electrospinning. *Acta Biomater.* **2010**, *6*, 4199−4207.
(154) Moreno, I.; González-González, V.; Romero-García, J. Control Release of Lactate Dehydrogenase Encapsulated in Poly (Vinyl Alcohol) Nanofibers via Electrospinning. *Eur. Polym. J.* **2011**, *47*, 1264−1272.
(155) Salalha, W.; Kuhn, J.; Dror, Y.; Zussman, E. Encapsulation of Bacteria and Viruses in Electrospun Nanofibres. *Nanotechnology* **2006**, *17*, 4675−4681.
(156) Jayasinghe, S. N.; Irvine, S.; McEwan, J. R. Cell Electrospinning Highly Concentrated Cellular Suspensions Containing Primary Living Organisms into Cell-Bearing Threads and Scaffolds. *Nanomedicine* **2007**, *2*, 555−567.
(157) Townsend-Nicholson, A.; Jayasinghe, S. N. Cell Electrospinning: A Unique Biotechnique for Encapsulating Living Organisms for Generating Active Biological Microthreads/Scaffolds. *Biomacromolecules* **2006**, *7*, 3364−3369.
(158) Cho, J.-S.; Kwon, A.; Cho, C.-G. Microencapsulation of Octadecane as a Phase-Change Material by Interfacial Polymerization in an Emulsion System. *Colloid Polym. Sci.* **2002**, *280*, 260−266.
(159) Hawlader, M. N. A.; Uddin, M. S.; Khin, M. M. Microencapsulated PCM Thermal-Energy Storage System. *Appl. Energy* **2003**, *74*, 195−202.
(160) Chang, C. C.; Tsai, Y. L.; Chiu, J. J.; Chen, H. Preparation of Phase Change Materials Microcapsules by Using PMMA Network-Silica Hybrid Shell via Sol-Gel Process. *J. Appl. Polym. Sci.* **2009**, *112*, 1850−1857.
(161) Kampeerapappun, P.; Phanomkate, N. Slow Release Fertilizer from Core-Shell Electrospun Fibers. *Chiang Mai J. Sci.* **2013**, *40*, 775−782.
(162) White, S. R.; Sottos, N. R.; Geubelle, P. H.; Moore, J. S.; Kessler, M. R.; Sriram, S. R.; Brown, E. N.; Viswanathan, S. Autonomic Healing of Polymer Composites. *Nature* **2001**, *409*, 794−797.
(163) Huang, Z. M.; Zhang, Y.; Ramakrishna, S. Double-Layered Composite Nanofibers and Their Mechanical Performance. *J. Polym. Sci., Part B: Polym. Phys.* **2005**, *43*, 2852−2861.
(164) Friend, J.; Yeo, L. Fabrication of Microfluidic Devices Using Polydimethylsiloxane. *Biomicrofluidics* **2010**, *4*, No. 026502.
(165) Yoo, B. Y.; Kim, B. H.; Lee, J. S.; Shin, B. H.; Kwon, H.; Koh, W. G.; Heo, C. Y. Dual Surface Modification of PDMS-Based Silicone Implants to Suppress Capsular Contracture. *Acta Biomater.* **2018**, *76*, 56−70.
(166) Lin, C.-H.; Yeh, Y.-H.; Lin, W.-C.; Yang, M.-C. Novel Silicone Hydrogel Based on PDMS and PEGMA for Contact Lens Application. *Colloids Surf., B* **2014**, *123*, 986−994.

https://dx.doi.org/10.1021/acsami.0c17706
ACS Appl. Mater. Interfaces 2021, 13, 48−66

(167) Schiffman, J. D.; Kiechel, M. A.; Donius, A. E.; Wegst, U. G. K.; Schauer, C. L. Crosslinking Poly(Allylamine) Fibers Electrospun from Basic and Acidic Solutions. *J. Mater. Sci.* **2013**, *48*, 7856−7862.
(168) Doan, T. Q.; Leslie, L. S.; Kim, S. Y.; Bhargava, R.; White, S. R.; Sottos, N. R. Characterization of Core-Shell Microstructure and Self-Healing Performance of Electrospun Fiber Coatings. *Polymer* **2016**, *107*, 263−272.
(169) Guarino, V.; Branda, F.; Ausanio, G.; Iannotti, V.; Lanotte, L.; Ambrosio, L. Elastomagnetic NI-PDMS Nanofibers via Coaxial Electrospinning. *Mater. Res. Express* **2018**, *5*, No. 085029.
(170) Lin, M. F.; Xiong, J.; Wang, J.; Parida, K.; Lee, P. S. Core-Shell Nanofiber Mats for Tactile Pressure Sensor and Nanogenerator Applications. *Nano Energy* **2018**, *44*, 248−255.
(171) Bedford, N. M.; Dickerson, M. B.; Drummy, L. F.; Koerner, H.; Singh, K. M.; Vasudev, M. C.; Durstock, M. F.; Naik, R. R.; Steckl, A. J. Nanofiber-Based Bulk-Heterojunction Organic Solar Cells Using Coaxial Electrospinning. *Adv. Energy Mater.* **2012**, *2*, 1136−1144.
(172) Yu, D. G.; Branford-White, C. J.; Chatterton, N. P.; White, K.; Zhu, L. M.; Shen, X. X.; Nie, W. Electrospinning of Concentrated Polymer Solutions. *Macromolecules* **2010**, *43*, 10743−10746.
(173) Larsen, G.; Spretz, R.; Velarde-Ortiz, R. Use of Coaxial Gas Jackets to Stabilize Taylor Cones of Volatile Solutions and to Induce Particle-to-Fiber Transitions. *Adv. Mater.* **2004**, *16*, 166−169.
(174) Lin, Y.; Yao, Y.; Yang, X.; Shen, L.; Li, R.; Wu, D. Effect of Gas Flow Rate on Crystal Structures of Electrospun and Gas-Jet/Electrospun Poly(Vinylidene Fluoride) (PVDF) Fibers. *Chin. J. Polym. Sci.* **2009**, *27*, 511−516.
(175) Wang, M.; Wang, K.; Yang, Y.; Liu, Y.; Yu, D.-G. Electrospun Environment Remediation Nanofibers Using Unspinnable Liquids as the Sheath Fluids: A Review. *Polymers* **2020**, *12*, 103.
(176) Yu, D. G.; Branford-White, C.; White, K.; Chatterton, N. P.; Zhu, L. M.; Huang, L. Y.; Wang, B. A Modified Coaxial Electrospinning for Preparing Fibers from a High Concentration Polymer Solution. *eXPRESS Polym. Lett.* **2011**, *5*, 732−741.
(177) Yu, D. G.; Zhu, L. M.; Bligh, S. W. A.; Branford-White, C.; White, K. N. Coaxial Electrospinning with Organic Solvent for Controlling the Size of Self-Assembled Nanoparticles. *Chem. Commun.* **2011**, *47*, 1216−1218.
(178) Yu, D. G.; Branford-White, C.; Bligh, S. W. A.; White, K.; Chatterton, N. P.; Zhu, L. M. Improving Polymer Nanofiber Quality Using a Modified Co-Axial Electrospinning Process. *Macromol. Rapid Commun.* **2011**, *32*, 744−750.
(179) Yu, D. G.; Li, X. Y.; Chian, W.; Li, Y.; Wang, X. Influence of Sheath Solvents on the Quality of Ethyl Cellulose Nanofibers in a Coaxial Electrospinning Process. *Bio-Med. Mater. Eng.* **2014**, *24*, 695−701.
(180) Yang, J. M.; Zha, L.; Yu, D. G.; Liu, J. Coaxial Electrospinning with Acetic Acid for Preparing Ferulic Acid/Zein Composite Fibers with Improved Drug Release Profiles. *Colloids Surf., B* **2013**, *102*, 737−743.
(181) Yan, J.; White, K.; Yu, D. G.; Zhao, X. Y. Sustained-Release Multiple-Component Cellulose Acetate Nanofibers Fabricated Using a Modified Coaxial Electrospinning Process. *J. Mater. Sci.* **2014**, *49*, 538−547.
(182) Wang, X.; Yu, D. G.; Li, X. Y.; Bligh, S. W. A.; Williams, G. R. Electrospun Medicated Shellac Nanofibers for Colon-Targeted Drug Delivery. *Int. J. Pharm.* **2015**, *490*, 384−390.
(183) Yu, D. G.; Yu, J. H.; Chen, L.; Williams, G. R.; Wang, X. Modified Coaxial Electrospinning for the Preparation of High-Quality Ketoprofen-Loaded Cellulose Acetate Nanofibers. *Carbohydr. Polym.* **2012**, *90*, 1016−1023.
(184) Yu, D. G.; Lu, P.; Branford-White, C.; Yang, J. H.; Wang, X. Polyacrylonitrile Nanofibers Prepared Using Coaxial Electrospinning with LiCl Solution as Sheath Fluid. *Nanotechnology* **2011**, *22*, 435301.
(185) Yu, D. G.; White, K.; Yang, J. H.; Wang, X.; Qian, W.; Li, Y. PVP Nanofibers Prepared Using Co-Axial Electrospinning with Salt Solution as Sheath Fluid. *Mater. Lett.* **2012**, *67*, 78−80.
(186) Yu, D. G.; Chatterton, N. P.; Yang, J. H.; Wang, X.; Liao, Y. Z. Coaxial Electrospinning with Triton X-100 Solutions as Sheath Fluids for Preparing PAN Nanofibers. *Macromol. Mater. Eng.* **2012**, *297*, 395−401.
(187) Yu, D. G.; Williams, G. R.; Gao, L. D.; Bligh, S. W. A.; Yang, J. H.; Wang, X. Coaxial Electrospinning with Sodium Dodecylbenzene Sulfonate Solution for High Quality Polyacrylonitrile Nanofibers. *Colloids Surf., A* **2012**, *396*, 161−168.
(188) Yu, D. G.; Li, X. Y.; Wang, X.; Chian, W.; Liao, Y. Z.; Li, Y. Zero-Order Drug Release Cellulose Acetate Nanofibers Prepared Using Coaxial Electrospinning. *Cellulose* **2013**, *20*, 379−389.
(189) Duan, G.; Greiner, A. Air-Blowing-Assisted Coaxial Electrospinning toward High Productivity of Core/Sheath and Hollow Fibers. *Macromol. Mater. Eng.* **2019**, *304*, 1800669.
(190) Lallave, M.; Bedia, J.; Ruiz-Rosas, R.; Rodríguez-Mirasol, J.; Cordero, T.; Otero, J. C.; Marquez, M.; Barrero, A.; Loscertales, I. G. Filled and Hollow Carbon Nanofibers by Coaxial Electrospinning of Alcell Lignin without Binder Polymers. *Adv. Mater.* **2007**, *19*, 4292−4296.
(191) Um, I. C.; Fang, D.; Hsiao, B. S.; Okamoto, A.; Chu, B. Electro-Spinning and Electro-Blowing of Hyaluronic Acid. *Biomacromolecules* **2004**, *5*, 1428−1436.
(192) Ahmad, B.; Stride, E.; Stoyanov, S.; Pelan, E.; Edirisinghe, M. Electrospinning of Ethyl Cellulose Fibres with a Heated Needle and Heated Air Using a Co-Axial Needle: A Comparison. *J. Med. Bioeng.* **2012**, *1*, 1−3.
(193) Choi, M.; Kim, J. Development of Coaxial Air-Blown Electrospinning Process for Manufacturing Non-Woven Nanofiber. I. Morphology Changes in Non-Woven Nanofiber. *Fibers Polym.* **2019**, *20*, 1601−1607.
(194) Kong, C. S.; Yoo, W. S.; Lee, K. Y.; Kim, H. S. Nanofiber Deposition by Electroblowing of PVA (Polyvinyl Alcohol). *J. Mater. Sci.* **2009**, *44*, 1107−1112.
(195) Pokorny, M.; Rassushin, V.; Wolfova, L.; Velebny, V. Increased Production of Nanofibrous Materials by Electroblowing from Blends of Hyaluronic Acid and Polyethylene Oxide. *Polym. Eng. Sci.* **2016**, *56*, 932−938.
(196) Liu, W.; Yao, Y.; Lin, Y.; Wang, B.; Luo, Y.; Li, N.; Zhang, Q.; Wu, Y.; Niu, A. J. Electrospinning Assisted by Gas Jet for Preparing Ultrafine Poly (Vinyl Alcohol) Fibres. *Iran. Polym. J.* **2009**, *18*, 89−96.
(197) Jiang, J.; Wang, X.; Li, W.; Liu, J.; Liu, Y.; Zheng, G. Electrohydrodynamic Direct-Writing Micropatterns with Assisted Airflow. *Micromachines* **2018**, *9*, 456.
(198) Balogh, A.; Horváthová, T.; Fülöp, Z.; Loftsson, T.; Harasztos, A. H.; Marosi, G.; Nagy, Z. K. Electroblowing and Electrospinning of Fibrous Diclofenac Sodium-Cyclodextrin Complex-Based Reconstitution Injection. *J. Drug Delivery Sci. Technol.* **2015**, *26*, 28−34.
(199) Zhmayev, Y.; Pinge, S.; Shoorideh, G.; Shebert, G. L.; Kaur, P.; Liu, H.; Joo, Y. L. Controlling the Placement of Spherical Nanoparticles in Electrically Driven Polymer Jets and Its Application to Li-Ion Battery Anodes. *Small* **2016**, *12*, 5543−5553.
(200) Paajanen, J.; Lönnrot, S.; Heikkilä, M.; Meinander, K.; Kemell, M.; Hatanpää, T.; Ainassaari, K.; Ritala, M.; Koivula, R. Novel Electroblowing Synthesis of Submicron Zirconium Dioxide Fibers: Effect of Fiber Structure on Antimony(v) Adsorption. *Nanoscale Adv.* **2019**, *1*, 4373−4383.
(201) Zhou, H.; Shi, Z.; Wan, X.; Fang, H.; Yu, D. G.; Chen, X.; Liu, P. The Relationships between Process Parameters and Polymeric Nanofibers Fabricated Using a Modified Coaxial Electrospinning. *Nanomaterials* **2019**, *9*, 843.
(202) Hong, K. H. Preparation and Properties of Electrospun Poly (Vinyl Alcohol)/Silver Fiber Web as Wound Dressings. *Polym. Eng. Sci.* **2007**, *47*, 43−49.
(203) Chou, W. L.; Yu, D. G.; Yang, M. C. The Preparation and Characterization of Silver-Loading Cellulose Acetate Hollow Fiber Membrane for Water Treatment. *Polym. Adv. Technol.* **2005**, *16*, 600−607.
(204) Xie, J.; Mao, H.; Yu, D. G.; Williams, G. R.; Jin, M. Highly Stable Coated Polyvinylpyrrolidone Nanofibers Prepared Using Modified Coaxial Electrospinning. *Fibers Polym.* **2014**, *15*, 78−83.

https://dx.doi.org/10.1021/acsami.0c17706
ACS Appl. Mater. Interfaces 2021, 13, 48−66

(205) Yu, D. G.; Chian, W.; Wang, X.; Li, X. Y.; Li, Y.; Liao, Y. Z. Linear Drug Release Membrane Prepared by a Modified Coaxial Electrospinning Process. *J. Membr. Sci.* **2013**, *428*, 150−156.
(206) Xu, Y.; Li, J. J.; Yu, D. G.; Williams, G. R.; Yang, J. H.; Wang, X. Influence of the Drug Distribution in Electrospun Gliadin Fibers on Drug-Release Behavior. *Eur. J. Pharm. Sci.* **2017**, *106*, 422−430.
(207) Rieger, K. A.; Schiffman, J. D. Electrospinning an Essential Oil: Cinnamaldehyde Enhances the Antimicrobial Efficacy of Chitosan/Poly(Ethylene Oxide) Nanofibers. *Carbohydr. Polym.* **2014**, *113*, 561−568.
(208) Nguyen, T. T. T.; Chung, O. H.; Park, J. S. Coaxial Electrospun Poly(Lactic Acid)/Chitosan (Core/Shell) Composite Nanofibers and Their Antibacterial Activity. *Carbohydr. Polym.* **2011**, *86*, 1799−1806.
(209) Kalwar, K.; Sun, W.-X.; Li, D.-L.; Zhang, X.-J.; Shan, D. Coaxial Electrospinning of Polycaprolactone@chitosan: Characterization and Silver Nanoparticles Incorporation for Antibacterial Activity. *React. Funct. Polym.* **2016**, *107*, 87−92.
(210) Han, D.; Steckl, A. J. Superhydrophobic and Oleophobic Fibers by Coaxial Electrospinning. *Langmuir* **2009**, *25*, 9454−9462.
(211) Muthiah, P.; Hsu, S.-H.; Sigmund, W. Coaxially Electrospun PVDF−Teflon AF and Teflon AF−PVDF Core−Sheath Nanofiber Mats with Superhydrophobic Properties. *Langmuir* **2010**, *26*, 12483−12487.

https://dx.doi.org/10.1021/acsami.0c17706
ACS Appl. Mater. Interfaces 2021, 13, 48−66